Title
Unconventional secretion of FABP4 by endosomes and secretory lysosomes

Journal
Journal of Cell Biology, 217(2)

ISSN
0021-9525

Authors
Villeneuve, Julien
Bassaganyas, Laia
Lepreux, Sebastien
et al.

Publication Date
2018-02-05

DOI
10.1083/jcb.201705047

Peer reviewed

Unconventional secretion of FABP4 by endosomes and secretory lysosomes

Julien Villeneuve,[1,2] Laia Bassaganyas,[3,4] Sebastien Lepreux,[5] Marioara Chiritoiu,[1] Pierre Costet,[6] Jean Ripoche,[5] Vivek Malhotra,[1,7,8] and Randy Schekman[2]

[1]Center for Genomic Regulation, Barcelona Institute of Science and Technology, Barcelona, Spain
[2]Department of Molecular and Cell Biology and Howard Hughes Medical Institute, University of California, Berkeley, Berkeley, CA
[3]Cardiovascular Research Institute and [4]Institute for Human Genetics, University of California, San Francisco, San Francisco, CA
[5]Institut National de la Santé et de la Recherche Médicale U1026 and [6]Service des Animaleries, Université de Bordeaux, Bordeaux, France
[7]Universitat Pompeu Fabra and [8]Institutio Catalana de Recerca i Estudis Avancats, Barcelona, Spain

An appreciation of the functional properties of the cytoplasmic fatty acid binding protein 4 (FABP4) has advanced with the recent demonstration that an extracellular form secreted by adipocytes regulates a wide range of physiological functions. Little, however, is known about the mechanisms that mediate the unconventional secretion of FABP4. Here, we demonstrate that FABP4 secretion is mediated by a membrane-bounded compartment, independent of the conventional endoplasmic reticulum–Golgi secretory pathway. We show that FABP4 secretion is also independent of GRASP proteins, autophagy, and multivesicular bodies but involves enclosure within endosomes and secretory lysosomes. We highlight the physiological significance of this pathway with the demonstration that an increase in plasma levels of FABP4 is inhibited by chloroquine treatment of mice. These findings chart the pathway of FABP4 secretion and provide a potential therapeutic means to control metabolic disorders associated with its dysregulated secretion.

Introduction

In eukaryotic cells, the vast majority of secreted proteins are first targeted to the ER via an N-terminal signal sequence and then exported to the Golgi apparatus, where they are sorted and delivered to their final destination by vesicular transport carriers (Schatz and Dobberstein, 1996; Lee et al., 2004). However, eukaryotic cells also secrete cytoplasmic proteins that do not contain an N-terminal signal sequence to enter the conventional secretory pathway. This class of secretory cargoes such as Acb1, superoxide dismutase-1 (SOD1), interleukin-1β (IL-1β), and insulin-degrading enzymes is mostly released in a cell type–dependent manner in association with specific environmental conditions and cellular stress (Kinseth et al., 2007; Nickel and Rabouille, 2009; Nickel, 2010; Rabouille et al., 2012; Malhotra, 2013; Zhang and Schekman, 2013).

The signal sequence–lacking FABP4 (or Adipocyte-FABP or Adipokin-2 [AP2]) is secreted by adipocytes subjected to lipolytic agonists or nutrient deprivation, and the secreted form is proposed to control glucose production by hepatocytes and insulin secretion by pancreatic β-cells (Cao et al., 2013; Kralisch et al., 2014; Wu et al., 2014; Ertunc et al., 2015; Hotamisligil and Bernlohr, 2015; Mita et al., 2015). It is also well documented that plasma levels of FABP4 are elevated in metabolic diseases such as obesity and type 2 diabetes mellitus (Xu et al., 2006; Tso et al., 2007; Cao et al., 2013; Kralisch et al., 2015). These disorders are associated with complex and reciprocal cross talk between immune and metabolic signaling, which ultimately leads to a chronic state of systemic metainflammation, dysregulation of adipocyte lipolysis, and alteration of liver glucose production (Gregor and Hotamisligil, 2011). In this context, targeting the secreted form of FABP4 may be a useful therapeutic approach. Indeed, it has been reported that administration of antibodies targeting FABP4 corrects a diabetic phenotype of obese mice by lowering fasting blood glucose, improving systemic glucose metabolism, increasing systemic insulin sensitivity, and reducing fat mass and liver steatosis (Cao et al., 2013; Burak et al., 2015).

But, how is FABP4 secreted? It has recently been reported that multivesicular bodies (MVBs) and exosomes contribute to FABP4 secretion (Ertunc et al., 2015). There are also studies of the existence of FABP4 in soluble form in the extracellular space (Lamounier-Zepter et al., 2009; Kralisch et al., 2014; Ertunc et al., 2015; Mita et al., 2015), which suggests the involvement of other routes for its release by cells.

Thus, beyond understanding fundamental cellular processes, deciphering how FABP4 is secreted and finding means to affect its secretion are potentially highly significant. We have monitored secretion of FABP4 in tissue culture cells and in mice, and our data reveal that FABP4 is mainly secreted by an endosomal/lysosomal pathway.

Correspondence to Randy Schekman: schekman@berkeley.edu; Vivek Malhotra: vivek.malhotra@crg.eu

The Rockefeller University Press
J. Cell Biol. Vol. 217 No. 2 649–665
https://doi.org/10.1083/jcb.201705047

Results

FABP4 secretion is induced by lipolytic agonists in adipocytes

We used 3T3-L1–derived adipocytes to address the pathway and mechanisms of FABP4 secretion (Fig. S1, A and B). Immunoblot analysis of cell lysates confirmed that FABP4 expression was strongly induced by differentiation of 3T3-L1 adipocytes (Fig. S1 C). Adipocytes secrete FABP4 in response to lipolytic agonist stimulation (Cao et al., 2013; Ertunc et al., 2015; Mita et al., 2015), so we first tested the effects of different lipolytic agonists on FABP4 secretion. Adipocytes were incubated in complete medium with increasing concentrations of forskolin (FSK) or 3-isobutyl-1-methylxanthine (IBMX), which are an adenylate cyclase activator and phosphodiesterase inhibitor, respectively. At the times indicated, fractions of the medium and cell lysates were immunoblotted with specific antibodies, which revealed that FSK and IBMX treatment increased FABP4 release into the culture medium. Approximately 50% of the total pool of FABP4 was detected in the medium after 1 h of incubation with 20 µM FSK or 500 µM IBMX (Fig. 1, A and B). No further increase in FABP4 secretion was detected after 2 h, suggesting FABP4 was secreted in a single burst (Fig. 1 C). An inactive analogue of FSK, 1,9-dideoxy-FSK (1,9-ddFSK), was inefficient in promoting FABP4 secretion (Fig. 1 D). Lipolytic stimulation of FABP4 secretion was differentiation-dependent. Although FABP4 was expressed by adipocytes at different time points of differentiation, it was only weakly secreted after 3 d but strongly secreted after 9 d of differentiation (Fig. S1 D). We also confirmed the induction of FABP4 secretion upon FSK treatment in mouse embryonic fibroblast (MEF)–derived adipocytes (Fig. S1, E–H). Under all conditions, α-tubulin was not detected in the medium, thus minimizing the possibility that cell lysis was the cause of FABP4 release. Cell viability was also confirmed for each condition by trypan blue dye exclusion (unpublished data).

FABP4 is not secreted via conventional secretory processes, MVBs/exosomes, or autophagy processes

We incubated adipocytes with FSK in the presence or absence of brefeldin A (BFA) or monensin, which inhibit the conventional ER-Golgi pathway of protein secretion. After 4 h of treatment with these chemicals, the medium and cell lysates tested by immunoblot revealed that ACDC, an adipocytokine secreted via the conventional secretory pathway, was strongly inhibited by BFA and monensin; however, FSK-induced FABP4 secretion was not impaired (Fig. 2 A).

Recent evidence suggested a role for MVBs and exosomes in the secretion of FABP4 (Ertunc et al., 2015). In this study, ∼5% of the total pool of secreted FABP4 was found within exosomes, suggesting that other mechanisms and secretory routes mediate FABP4 release. We retested this proposal. Adipocytes were incubated with FSK in complete medium for 4 h, and the medium was subjected to differential centrifugations to collect exosomes. The membrane pellet and soluble supernatant fractions were analyzed by SDS-PAGE and immunoblotting. CD63, an exosomal marker, was exclusively detected in the 100,000 *g* centrifuged pellet fraction, whereas ACDC and FABP4 were largely detected in the soluble fraction (Fig. 2 B). To further examine a possible role of MVBs and exosomes in FABP4 secretion, genes encoding Hrs and TSG101, two essential components of endosomal sorting complex required for transport-mediated production of MVBs, were depleted using the CRISPR/Cas9 approach (Cong et al., 2013; Mali et al., 2013). Immunoblot analysis revealed that FSK-induced FABP4 secretion was not altered in adipocytes depleted of Hrs or TSG101 compared with wild-type cells (Fig. 2, C and D). These results strongly suggest that FABP4 secretion does not depend on MVBs and exosomes.

Cytoplasmic proteins such as Acb1 in yeast (Duran et al., 2010; Manjithaya et al., 2010) and IL-1β in mammalian cells (Dupont et al., 2011; Zhang et al., 2015) are reported to require autophagy-related genes (Atg) for their secretion. Is FABP4 secretion dependent on the function of Atg genes? We tested this possibility using inhibitors of phosphatidylinositol 3–kinase (PI3K), which is required to initiate the formation of autophagosomes (Klionsky et al., 2012). Treatment of adipocytes with wortmannin and 3-methyladenine, two well-known PI3K inhibitors, had no effect on FSK-induced FABP4 secretion (Fig. 2, E and F). We further tested the involvement of autophagy-mediated release of FABP4 in MEF cells lacking the ATG5 gene, which is necessary to initiate autophagy (Mizushima et al., 2001). Wild-type and ATG5 knockout MEF cells were transfected with Flag-FABP4 and incubated in starvation medium (Earle's Balanced Salt Solution [EBSS]), a condition reported to stimulate the secretion of other unconventionally secreted proteins (Duran et al., 2010; Bruns et al., 2011; Dupont et al., 2011; Zhang et al., 2015). Lipolytic agonist stimulation did not induce FABP4 secretion in MEF cells (unpublished data). Immunoblot analysis of cell lysates and the culture medium showed that cells incubated with EBSS stimulated FABP4 secretion in time-dependent manner. The autophagy process was abolished in *ATG5* knockout cells as shown by the absence of phosphatidylethanolamine-lipidated LC3, a key intermediate in autophagosome biogenesis. However, FABP4 secretion was not affected in *ATG5* knockout cells (Fig. 2 G). We also tested the role of the ER–Golgi intermediate compartment (ERGIC), which was identified as a membrane source for autophagosome biogenesis, in secretion of FABP4 (Ge et al., 2013). The formation of ERGIC is inhibited by high concentrations of H89 and clofibrate (Clo; Ge et al., 2013; Fig. S2 A), but such conditions did not affect FSK-induced FABP4 secretion (Fig. 2 H and Fig. S2 B). Altogether, these results suggested that autophagy is not required for FABP4 secretion.

Grh1 in yeast and its mammalian orthologues GRASP55 and GRASP65 are involved in unconventional secretion (Kinseth et al., 2007; Levi and Glick, 2007; Duran et al., 2010; Manjithaya et al., 2010; Giuliani et al., 2011; Cruz-Garcia et al., 2017). As shown in Fig. S2 (C and D), CRISPR/Cas9-mediated *GRASP55* and *GRASP65* knockout, however, did not impair FABP4 secretion. We therefore conclude that FABP4 release is independent of the GRASP proteins.

FABP4 secretion is mediated by secretory lysosomes

FABP4 secretion is stimulated by an increase in intracellular calcium (Kralisch et al., 2014; Schlottmann et al., 2014). Interestingly, this also promotes fusion of secretory lysosomes to the plasma membrane (Rodríguez et al., 1997; Reddy et al., 2001). To test whether secretory lysosomes are involved in FABP4 secretion, we tested the effects of chloroquine (CQ) and ammonium chloride, which block protein trafficking into lysosomes by raising their intraluminal pH (Tapper and Sundler, 1990;

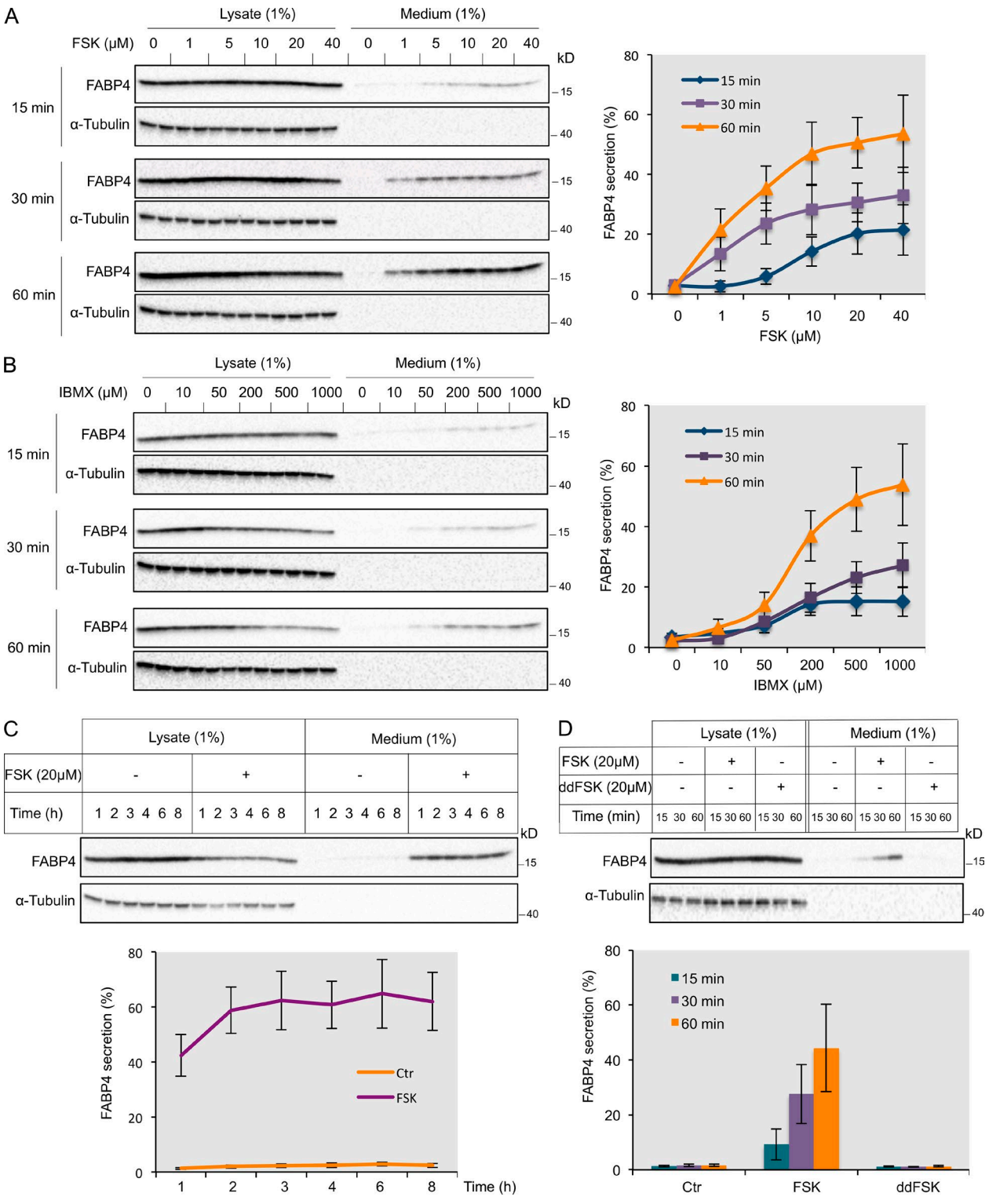

Figure 1. **FABP4 secretion is induced by lipolytic agonists in adipocytes. (A and B)** Left: Adipocytes were incubated with increasing concentrations of FSK (A) and IBMX (B) and at the indicated time, medium fractions were collected and cells lysed. For each condition, performed in duplicate, 1% of total cell lysate and medium was analyzed by immunoblotting with anti-FABP4 and anti–α-tubulin antibodies. Right: Quantification of FABP4 secretion. Results are shown as the mean ± SD of three independent experiments. **(C)** Top: Adipocytes were incubated with or without 20 μM FSK and at indicated times, media fractions were collected and cells lysed. For each time point, 1% of total cell lysate and medium was analyzed by immunoblotting with anti-FABP4 and anti–α-tubulin antibodies. Bottom: Quantification of FABP4 secretion. Results are shown as the mean ± SD of three independent experiments. **(D)** Top: Adipocytes were incubated with 20 μM FSK or 20 μM 1,9-ddFSK and at the indicated time, medium was collected and cells lysed. For each condition, 1% of total cell lysate and medium was analyzed by immunoblotting with anti-FABP4 and anti–α-tubulin antibodies. Bottom: Quantification of FABP4 secretion. Results are shown as the mean ± SD of three independent experiments. **(A–D)** FABP4 secretion was calculated as a percentage of the signal detected in the medium compared with the total amount (the sum of FABP4 in both medium and lysate).

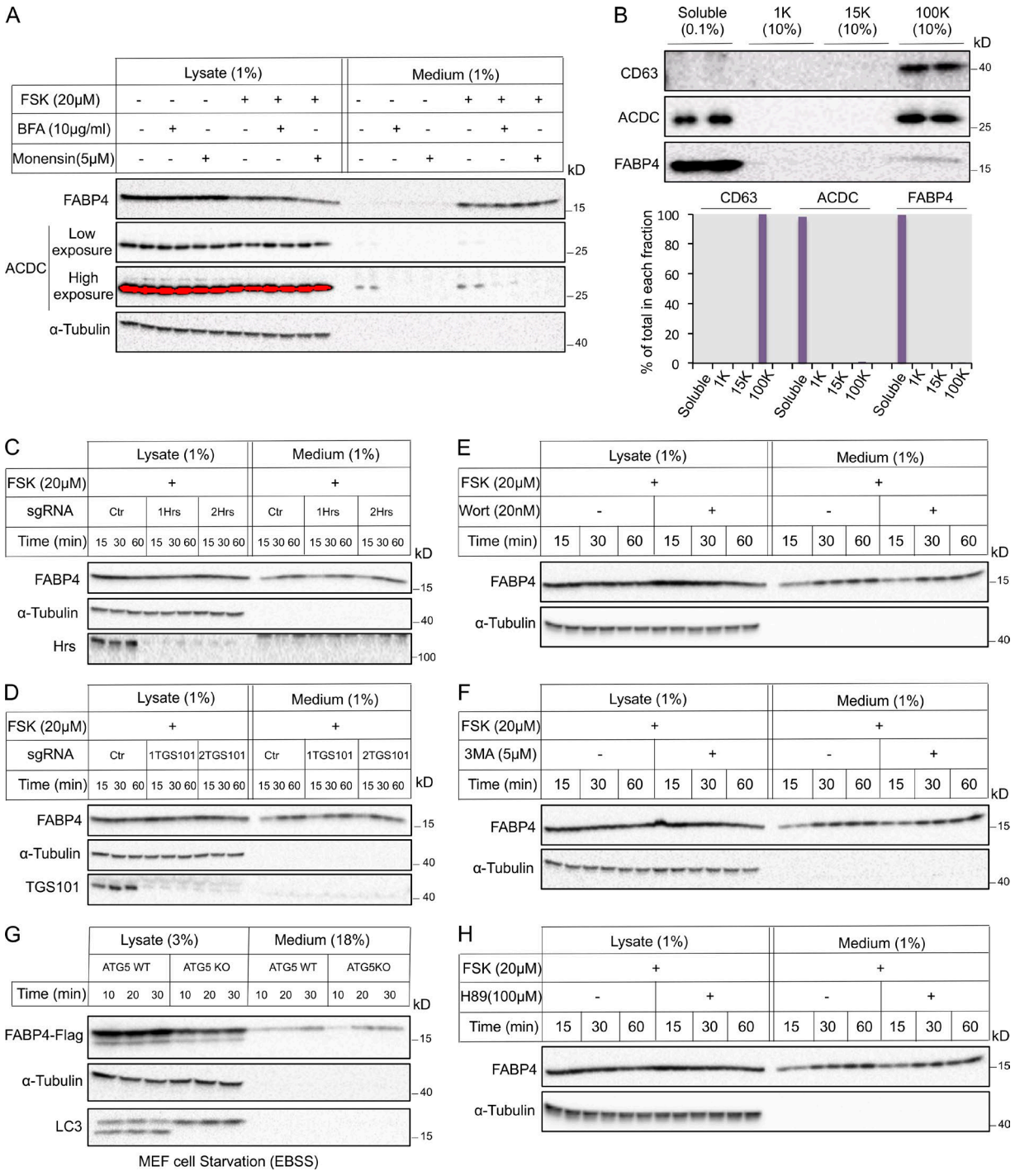

Figure 2. **FABP4 secretion is independent of conventional secretory pathway, autophagy processes, and MVBs, and is not secreted in exosomes.** **(A)** Adipocytes were incubated in the presence or absence of 20 µM FSK, 10 µg/ml BFA, or 5 µM monensin for 2 h. The medium fractions were collected and cells lysed, and for each condition, performed in duplicate, 1% of total cell lysate and medium was analyzed by immunoblotting with anti-FABP4, anti-ACDC, and anti–α-tubulin antibodies. **(B)** Top: Adipocytes were incubated with 10 µM FSK for 4 h, and the medium fraction was harvested and subjected to differential centrifugation. An aliquot (10%) of each membrane pellet fraction and 0.1% of the soluble fraction were analyzed by immunoblotting with anti-CD63, anti-ACDC, and anti-FABP4 antibodies. Bottom: Quantification of the percentage of the indicated protein in each fraction compared with the total expression. Results are representative of two independent experiments. **(C and D)** Wild-type adipocytes and adipocytes depleted for Hrs (C) and TSG101 (D) using the CRISPR/Cas9 system were incubated with 20 µM FSK, and at indicated times, medium fractions were collected and cells lysed. For each condition, 1% of total cell lysate and medium was analyzed by immunoblotting with anti-FABP4 and anti–α-tubulin antibodies. Gene disruption efficiencies were validated by immunoblotting with anti-Hrs (C) and anti-TSG101 (D) antibodies. **(E, F, and H)** Adipocytes were incubated with 20 µM FSK in the presence or absence of 20 nM wortmannin (Wort; E), 5 µM PI3K inhibitor 3-methyladenin (3MA; F) or 100 µM H89 (H), and at indicated times, medium fractions were collected and cells lysed. For each condition, performed in duplicate, 1% of total cell lysate and medium fractions was analyzed by immunoblotting with anti-FABP4 and anti–α-tubulin antibodies. **(G)** Wild-type and knockout (KO) *ATG5* MEF cells were transfected to express Flag-FABP4 and incubated in EBSS. At the indicated time, cells were lysed and medium fractions were concentrated using TCA precipitation. For each condition, 3% of the total cell lysate and 18% of the medium were analyzed by immunoblotting with anti-Flag, anti–α-tubulin and anti-LC3 antibodies.

Ling et al., 1998; Andrei et al., 1999; Luo et al., 2011). The level of phosphatidylethanolamine-LC3 and P62, two proteins targeted to lysosomes for degradation by autophagy, accumulated in cells incubated with CQ and ammonium chloride, demonstrating the efficiency of these drugs. Correspondingly, CQ and ammonium chloride treatment strongly inhibited FSK-induced FABP4 secretion and caused intracellular accumulation of FABP4 (Fig. 3, A and B). We also confirmed the effect of CQ on FSK-induced FABP4 secretion using MEF-derived adipocytes (Fig. S3 A). We then tested the effect of concanamycin A and bafilomycin A1, two other drugs that raise the lysosomal pH by inhibition of the vacuolar H^+ adenoside triphophatase (Bowman et al., 1988; Kataoka et al., 1994; Yamamoto et al., 1998), on FABP4 secretion. Treatment of adipocytes with concanamycin A or bafilomycin A1 also inhibited FSK-induced FABP4 secretion (Fig. S3, B and C).

These results suggested that the lysosomal compartment was involved in FABP4 secretion. LAMP1 is a specific lysosomal marker expressed at the plasma membrane after lysosomal exocytosis. We tested whether FSK stimulation triggered lysosomal exocytosis by monitoring its effect on LAMP1 expression at the cell surface by immunofluorescence and flow cytometry. Adipocytes incubated with FSK demonstrated the expression of LAMP1 at the cell surface (Fig. 3, C and D).

To further ascertain the involvement of fusion of FABP4-containing lysosomes to the plasma membrane, we tested the requirement of the specific fusion proteins VAMP-7 and synaptotagmin VII (SytVII; Martinez et al., 2000; Reddy et al., 2001; Rao et al., 2004). CRISPR/Cas9 mutations in *VAMP7* and *SytVII* loci were created by standard procedures, and wild-type and mutant adipocytes were treated with FSK. At the indicated times, media fractions were harvested and cells lysed. Immunoblot analysis revealed that knockout of *VAMP-7* and *SytVII* reduced FABP4 secretion, confirming the involvement of lysosomal exocytosis in FABP4 release to the extracellular space (Fig. 3, E and F).

Vesicular intermediates are required for FABP4 import into secretory lysosomes

It has been previously reported that cytosplasmic proteins such as heat shock protein 70 (HSP70), aldo-keto reductase family 1 member B8 (AKR1B8), and AKR1B10 are released in the extracellular space via secretory lysosomes (Mambula and Calderwood, 2006; Luo et al., 2011; Tang et al., 2014). Their translocation from cytoplasm into lysosomes is proposed to be mediated by ATP-binding cassette (ABC) transporters. Chemical inhibition of theses transporters reduced HSP70, AKR1B8, and AKR1B10 secretion (Mambula and Calderwood, 2006; Luo et al., 2011; Tang et al., 2014). Is FABP4 translocated from cytoplasm into lysosomes by ABC transporters? To test this, we stimulated adipocytes with FSK in the presence or absence of glibenclamide, a general ABC transporter inhibitor, and more selective inhibitors: 4,4'-diisothiocyanostilbene-2,2'-disulfonic acid (DIDS) and bromosulphalein (BSP). We tested the efficiency of these drugs on HSP70 secretion and confirmed the published findings (Mambula and Calderwood, 2006; Fig. S4 A). However, these inhibitors did not affect FABP4 secretion, suggesting that FABP4 was not translocated into lysosomes by ABC transporters (Fig. S4 B). We cannot exclude the possibility that other transmembrane proteins promote direct translocation of FABP4 into secretory lysosomes.

Another possibility is the involvement of upstream vesicular carriers, e.g., endosomes, containing FABP4 that fuse with lysosomes. In that case, such a prelysosomal carrier of FABP4 should accumulate in presence of lysosomotropic drugs such as CQ. We first tested this hypothesis by subcellular fractionation experiments. Total membranes and cytosol from adipocytes incubated in the presence or absence of FSK, with or without CQ, were separated by centrifugation. In control conditions, FABP4 was mainly detected in the cytosol fraction. In the presence of FSK, the FABP4 signal in the cytosolic fraction decreased, and a low level was detected in the membrane fraction. In the presence of FSK and CQ, however, the FABP4 signal decreased in the cytosol and accumulated in the sedimentable, presumably membrane-bound, fraction (Fig. 4 A). To verify that an equal amount of sedimentable membrane material was analyzed, we quantified phosphatidylcholine (PC) content for each condition and used other membrane markers such as ERGIC53, Sec22b, and LAMP1 as SDS-PAGE and immunoblot loading controls. Our findings revealed that CQ inhibition of FSK-induced FABP4 secretion correlated with accumulation of FABP4 in sedimentable membrane-bounded compartments. To extend these results, we resolved the total membrane pellet fraction from adipocytes incubated with FSK and CQ on a Nycodenz density gradient and analyzed FABP4 distribution in relation to other cellular compartments that contained ERGIC53 and Sec22b (ERGIC), GM130 (cis Golgi membrane), or protein disulfide isomerase (ER). FABP4 was detected in the buoyant density fractions 1 and 2, consistent with its association to membranes (Fig. 4 B). We also tested the protease sensitivity of the total membrane fraction containing FABP4. As a control, we first subjected medium-containing FABP4 to proteinase K. Proteinase K degraded FABP4 in the absence or presence of detergent (Fig. 4 C), demonstrating that FABP4 is secreted in a soluble form and not sequestered within microvesicles such as exosomes. In the same conditions, treatment of the membrane pellet fraction revealed that the SNARE protein Sec22b was proteinase K–sensitive with or without detergent, whereas ERGIC53, a lumenally exposed membrane protein, was proteinase K–sensitive only in the presence of detergent. Analysis of the total membrane fraction revealed that FABP4 was resistant to 50 µg/ml of proteinase K except in the presence of detergent (Fig. 4 C). We thus conclude that CQ inhibition of FSK-induced secretion results in accumulation of FABP4 in a membrane compartment.

We then fractionated membranes in an effort to identify the intracellular location of FABP4. For this purpose, we performed a three-step membrane fractionation procedure as previously described (Ge et al., 2013) and illustrated in Fig. 4 D. First, we conducted differential centrifugation to obtain three membrane pellet fractions and cytosol from lysates of adipocytes incubated in presence or absence of FSK with or without CQ. As demonstrated in Fig. 4 A, the FABP4 signal in the cytosol fraction decreased in adipocytes treated with FSK, with or without CQ, compared with a control condition. In the differential centrifugation fractions, we observed enrichment of FABP4 in the 25,000 *g* centrifuged (25k) pellet material obtained from adipocytes stimulated with FSK and CQ (Fig. 4 E). To further fractionate the 25k membrane fraction, we performed a sucrose step gradient ultracentrifugation (Fig. 4 D). This separated the 25k membrane into two distinct fractions: a light fraction between the 1.1 and 0.25 M layers of sucrose and the sedimented pellet fraction. In cells treated with FSK and CQ, the FABP4 signal

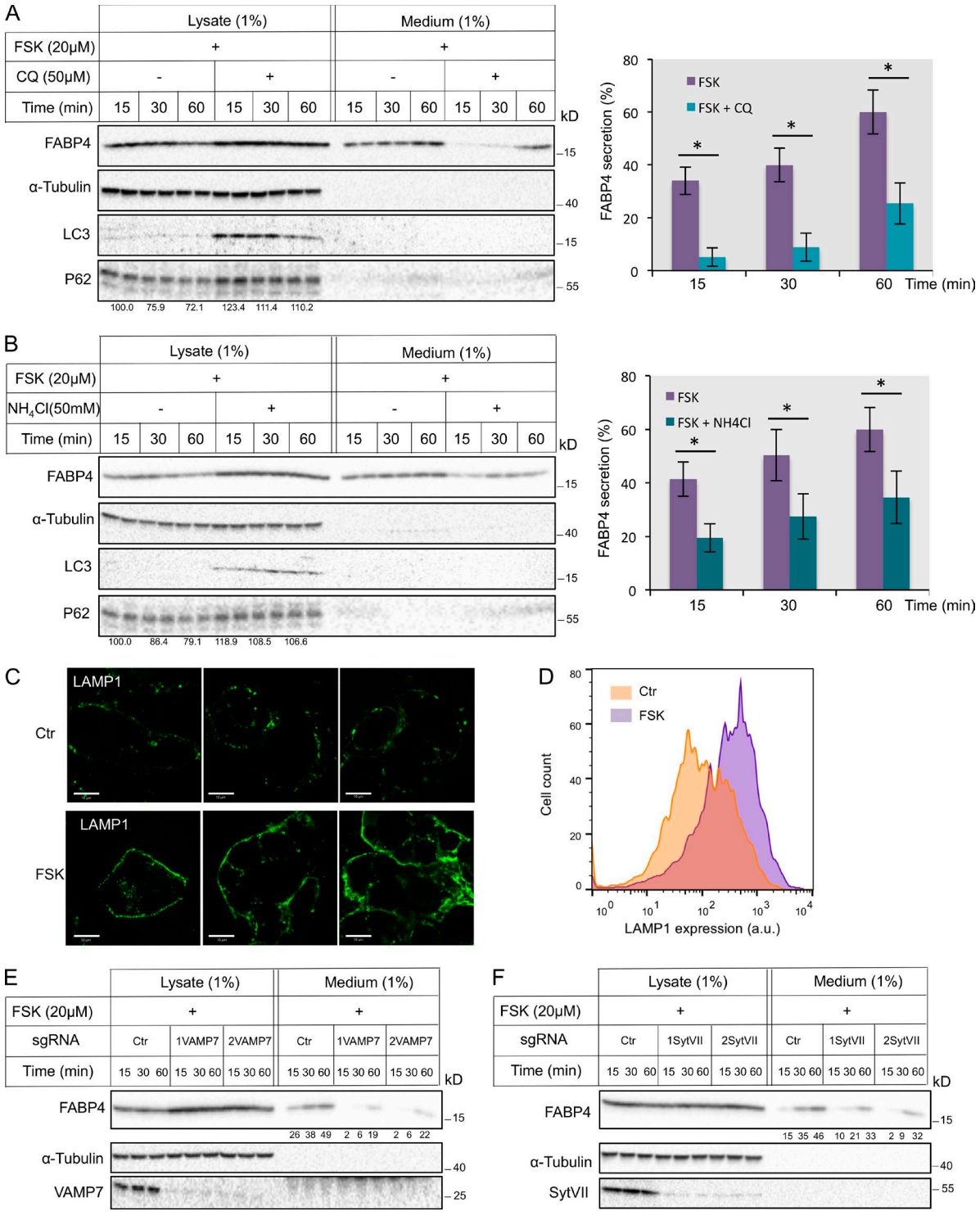

Figure 3. **FABP4 secretion is mediated by secretory lysosomes. (A and B)** Left: Adipocytes were incubated with 20 µM FSK in the presence or absence of 50 µM CQ (A) or 50 mM ammonium chloride (NH_4Cl; B), and at indicated times, medium fractions were collected and cells lysed. For each condition, performed in duplicate, 1% of total cell lysate and medium was analyzed by immunoblotting with anti-FABP4, anti–α-tubulin, anti-LC3, and anti-P62 antibodies. Quantification of P62 expression in cell lysates is indicated. Right: Quantification of FABP4 secretion. For each condition, FABP4 secretion was calculated as a percentage of the signal detected in the medium compared with the total amount (the sum of FABP4 in both medium and lysate). Results are shown as the mean ± SD of three independent experiments. *, $P < 0.05$. **(C and D)** Adipocytes were incubated with or without 20 µM FSK for 2 h, and LAMP1 expression at the cell surface was analyzed by immunofluorescence microscopy (C) and flow cytometry (D). For immunofluorescence microscopy analysis, three inserts are shown for each condition. Bar, 10 µm. For flow cytometry analysis, results are representative of three independent experiments. **(E and F)** Wild-type adipocytes and adipocytes depleted for VAMP7 (E) and SytVII (F) using the CRISPR/Cas9 system were incubated with 20 µM FSK, and at the indicated time, medium was collected and cells lysed. For each condition, 1% of total cell lysate and medium was analyzed by immunoblotting with anti-FABP4 and anti–α-tubulin antibodies. Knockout efficiencies were validated by immunoblotting with anti-VAMP7 (E) and anti-SytVII (F) antibodies. Quantification of FABP4 secretion was performed as described in A and B. Results are representative of three independent experiments. Ctr, control.

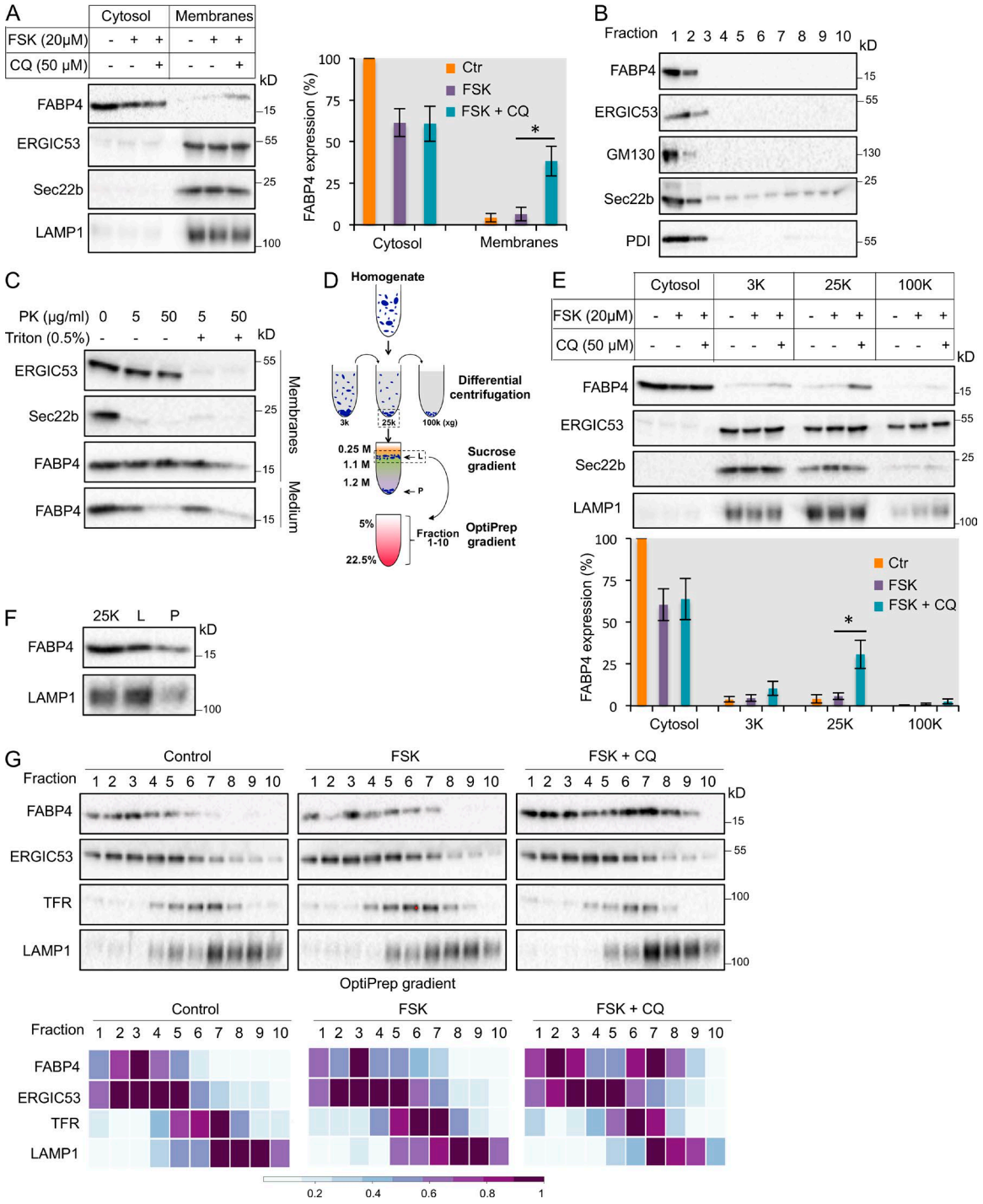

Figure 4. **FABP4 accumulates in membrane compartments when FSK-induced FABP4 secretion is inhibited with CQ. (A)** Left: Adipocytes were incubated in the presence or absence of 20 μM FSK with or without 50 μM CQ for 1 h. Adipocytes were homogenized, and the lysates were centrifuged to separate cytosol from the total membrane fraction. The total PC content of each membrane fraction was measured to sample the same amount of membranes for each condition. Cytosol and membrane fractions were analyzed by immunoblotting with anti-FABP4, anti-ERGIC53, anti-Sec22, and anti-LAMP1 antibodies. Right: Quantification of FABP4 expression. FABP4 expression was calculated as a percentage of the signal detected in each fraction compared with the signal detected in the cytosolic fraction in the control condition. Results are shown as the mean ± SD of three independent experiments. *, $P < 0.05$. **(B)** Adipocytes were incubated in the presence of 20 μM FSK with 50 μM CQ for 1 h. Adipocytes were homogenized, and the lysate was centrifuged to separate cytosol from the total membrane fraction. The total membrane fraction was subjected to Nycodenz density gradient centrifugation, after which 10 fractions were collected from the top and the indicated markers were detected by immunoblotting. **(C)** Adipocytes were incubated in the presence of 20 μM FSK with 50 μM CQ for 1 h. Medium was collected, adipocytes were homogenized, and the lysate was centrifuged to separate cytosol from the total membrane fraction. Medium and total membrane fractions were subjected to proteinase K treatment (see Materials and methods section) in the presence or absence of detergent, and specific marker proteins were analyzed by immunoblotting. **(D)** Membrane fractionation scheme. Adipocytes were homogenized, and the lysate was subjected to differential centrifugations. A first centrifugation at 1,000 *g* (1K) removed unbroken cells and nuclei. The first supernatant fraction was subjected successively to centrifugation at 3,000 *g* (3K), 25,000 *g* (25K), and 100,000 *g* (100K). The 25K pellet fraction, which had the highest level of FABP4, was selected, and a sucrose gradient ultracentrifugation was performed to separate the 25K pellet into L (light) and

was contained predominantly in the light fraction (Fig. 4 F). To further refine the membrane with which FABP4 associated, we centrifuged the light fraction on an OptiPrep gradient and collected 10 fractions from the top (Fig. 4 D). Immunoblotting with an anti-FABP4 antibody revealed a similar distribution when adipocytes were cultured in the control condition or with FSK: FABP4 was mainly distributed in fractions one through five (Fig. 4 G). However, upon incubation with FSK and CQ, an additional pool of FABP4 was found in fractions 6 through 8 coincident with the endosomal and lysosomal markers, transferrin receptor, and LAMP1, respectively (Fig. 4 G). Our fractionation results suggest that blocking FABP4 trafficking by CQ treatment causes its accumulation in a membrane-bounded compartment, possibly an endosome or endosome-associated lysosome.

FABP4 is successively transported in endosomal and lysosomal compartments for its secretion

We then explored the identity of FABP4-containing transport intermediates by immunofluorescence microscopy. In adipocytes incubated in the presence or absence of FSK with or without CQ, FABP4 localized throughout the cytoplasm (Fig. 5 A). To test whether a membrane-associated pool of FABP4 was masked by its predominant cytoplasmic form, adipocytes were permeabilized with saponin, washed extensively to remove the cytoplasmic protein, and then fixed for immunofluorescence microscopy with anti-FABP4 antibody. This approach revealed that FABP4 localized in punctate structures in cells treated with FSK and CQ (Fig. 5 B). This punctate pool of FABP4 did not colocalize with Golgi markers GM130 and GRASP65 or the early endosomal marker EEA1 (Fig. S5). We observed FABP4 location partially overlapped with LAMP1 (Fig. 5 C). For a more precise localization, we used structured illumination microscopy (SIM) and found that FABP4 was mainly distributed in close proximity to lysosomes marked by the membrane protein LAMP1 (Fig. 5 D, arrows). In some cells, FABP4 labeling appeared to be surrounded by LAMP1-containing membranes (Fig. 5 D, arrowhead). Some punctae of FABP4 also colocalized with mannose-6–phosphate receptor (M6PR) and Rab7, which are late endosomal markers (Fig. 5, E and F), suggesting that FABP4 may traffic through endosomal membranes en route to lysosomes.

To evaluate the role of endocytic pathway in FABP4 trafficking and secretion, we examined the effect of dynasore on adipocytes treated with FSK. Dynasore is an inhibitor of the guanosine triphosphatase dynamins 1 and 2 (Macia et al., 2006), which are essential for the scission of clathrin-coated vesicles that bud from the plasma membrane, the trans-Golgi network, and endosomes (Stoorvogel et al., 1996; Marsh and McMahon, 1999; Nicoziani et al., 2000; van Dam and Stoorvogel, 2002; Praefcke and McMahon, 2004). Immunoblot analysis revealed that in a dose-dependent manner at concentrations effective in blocking dynamin function in cells (Macia et al., 2006), dynasore strongly inhibited FABP4 secretion (Fig. 6, A and B). By immunofluorescence analysis, we found that dynasore affected colocalization of FABP4 with M6PR and LAMP1 (Fig. 6, C and D, respectively), and instead resulted in the colocalization of FABP4 with EEA1, which is an early endosomal marker (Fig. 6 E). In this condition, FABP4 did not colocalize with CD63, an MVB marker, and GRASP65 or GM130, Golgi membrane markers (Fig. 6, F–H). Although dynasore is not a specific inhibitor of dynamin, these results suggest that endosomal membranes are likely intermediates in the trafficking of FABP4 to lysosomes.

CQ treatment inhibits FABP4 secretion in mice

The finding that CQ inhibited FSK-induced FABP4 secretion in cultured adipocytes prompted us to test this finding in vivo. It was previously demonstrated that mice receiving isoproterenol, a mediator of lipolysis acting as β-adrenergic receptor agonist, exhibit a rapid increase in plasma FABP4 levels compared with vehicle-treated mice (Cao et al., 2013). Does CQ treatment inhibit FABP4 secretion in mice stimulated with lipolytic agents? We first tested the effect of isoproterenol on FABP4 secretion in cultured adipocytes. Adipocytes were incubated in complete medium with increasing concentrations of isoproterenol, and at the indicated times, aliquots of medium were harvested and cells lysed. Immunoblot analysis revealed that isoproterenol treatment stimulated FABP4 secretion (Fig. 7 A). Incubation with CQ strongly inhibited isoproterenol-induced FABP4 secretion, as shown in Fig. 7 B. We then tested this effect in mice. As reported earlier (Cao et al., 2013), we confirmed that plasma FABP4 levels increased rapidly 20 min after isoproterenol administration, after which FABP4 levels decreased, suggesting clearance from the bloodstream as a result of FABP4 secretion in a single burst (Fig. 7 C). We then tested the effect of CQ administered to mice 24 h and 1 h before isoproterenol. In these conditions, we observed that CQ pretreatment resulted in a significant decrease of plasma FABP4 concentration, demonstrating that CQ inhibited FABP4 release in the bloodstream (Fig. 7 D).

Discussion

FABP4, a cytoplasmic protein, is secreted by adipocytes, and in the extracellular space contributes to the progression of meta-

P (pellet) fractions. The L fraction, which contained the majority of FABP4, was further resolved on an OptiPrep gradient, after which 10 fractions were collected from the top. **(E)** Top: Adipocytes were incubated in the presence or absence of 20 µM FSK with or without 50 µM CQ for 1 h. Adipocytes were homogenized, and a differential centrifugation experiment was performed as depicted in D. The total PC content of each membrane fraction was measured to sample the same amount of membranes for each condition. Expression of FABP4 and the indicated membrane markers was analyzed in the cytosol and membrane fractions by immunoblotting. Bottom: Quantification of FABP4 expression. FABP4 expression was calculated as a percentage of the signal detected in each fraction compared with the signal detected in the cytosolic fraction in the control condition. Results are shown as the mean ± SD of three independent experiments. *, $P < 0.05$. **(F)** A sucrose step gradient ultracentrifugation to further separate the 25K pellet fraction was performed as depicted in D from adipocytes incubated in the presence of 20 µM FSK with 50 µM CQ for 1 h. The total PC content of each membrane fraction was measured to sample the same amount of membranes, and FABP4 and LAMP1 were detected by immunoblotting. **(G)** Top: OptiPrep gradient ultracentrifugation was used to resolve membranes in the L fraction as depicted in D from adipocytes incubated in the presence or absence of 20 µM FSK with or without 50 µM CQ for 1 h. 10 fractions were collected, and the total PC content of each membrane fraction was measured to sample the same amount of membranes, and FABP4 and specific membrane markers were analyzed by immunoblotting. Bottom: Heat maps showing the relative expression of FABP4, ERGIC, Transferrin receptor, and LAMP1. For each condition and each marker, the fraction with the highest value was defined as 1. Results are representative of three independent experiments.

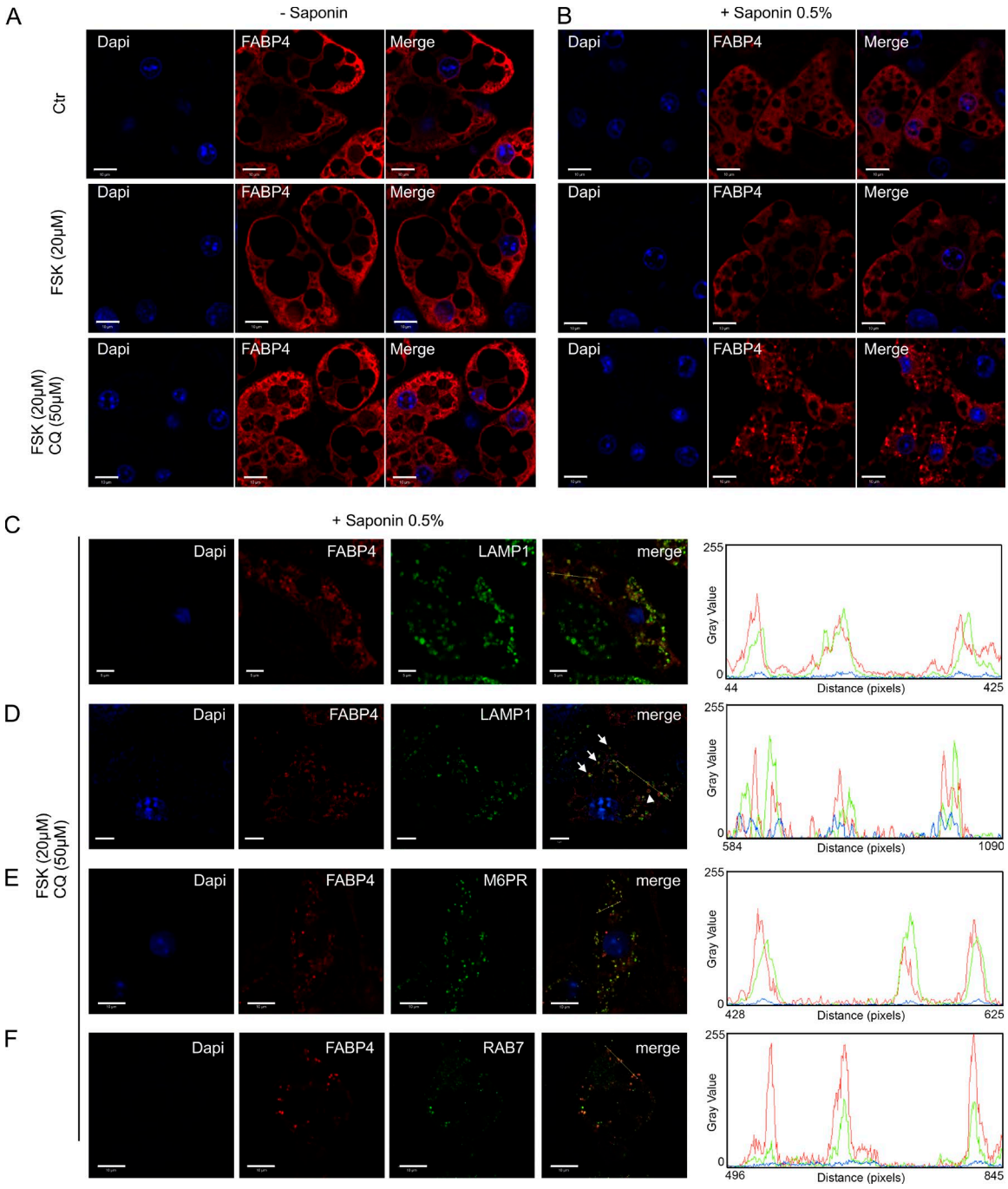

Figure 5. **FABP4 localizes in the endosomal/lysosomal compartment when FSK-induced FABP4 secretion is inhibited with CQ. (A and B)** Adipocytes were incubated in the presence or absence of 20 µM FSK with or without 50 µM CQ for 30 min. The localization of FABP4 was monitored by immunofluorescence microscopy in cells permeabilized or not with saponin before fixation. Bar, 10 µm. **(C–F)** Left: Adipocytes were incubated in the presence of 20 µM FSK with 50 µM CQ for 30 min, and cells were permeabilized with saponin before fixation. The colocalization of FABP4 with the indicated membrane markers was monitored by immunofluorescence microscopy. Bars: (C and D) 5 µm; (E and F) 10 µm. **(D)** Colocalization analysis using SIM. The close proximity between FABP4 and LAMP1 labeling is indicated by arrows and by an arrowhead identifying FABP4 labeling surrounded by LAMP1 labeling. Pearson correlation coefficient (r) of colocalization, FABP4/LAMP1 r: 0.317 (C); FABP4/LAMP1 r: 0.182 (D); FABP4/M6PR r: 0.530 (E); FABP4/RAB7 r: 0.456 (F); *n* = 10 for each colocalization analysis. Right: Intensity profile graphs of FABP4 colocalization with the indicated membrane markers.

bolic disease in a manner that is mitigated by anti-FABP4 antibodies (Cao et al., 2013; Burak et al., 2015). This suggests that inactivating extracellular FABP4 and/or blocking its export could have therapeutic potential.

Our findings show that FABP4 is secreted by adipocytes stimulated with lipolytic agonists independent of the classical secretory pathway and autophagy. Although MVB and exosomes have been implicated in FABP4 release (Ertunc et al., 2015), our data reveal that exosomes are not a primary means by which FABP4 is secreted. Rather, secretion appears to involve an endosome that may fuse or mature into secretory lysosomes, and then fuse with the plasma membrane in a calcium-dependent manner, thus releasing FABP4 to the extracellular space (Fig. 8).

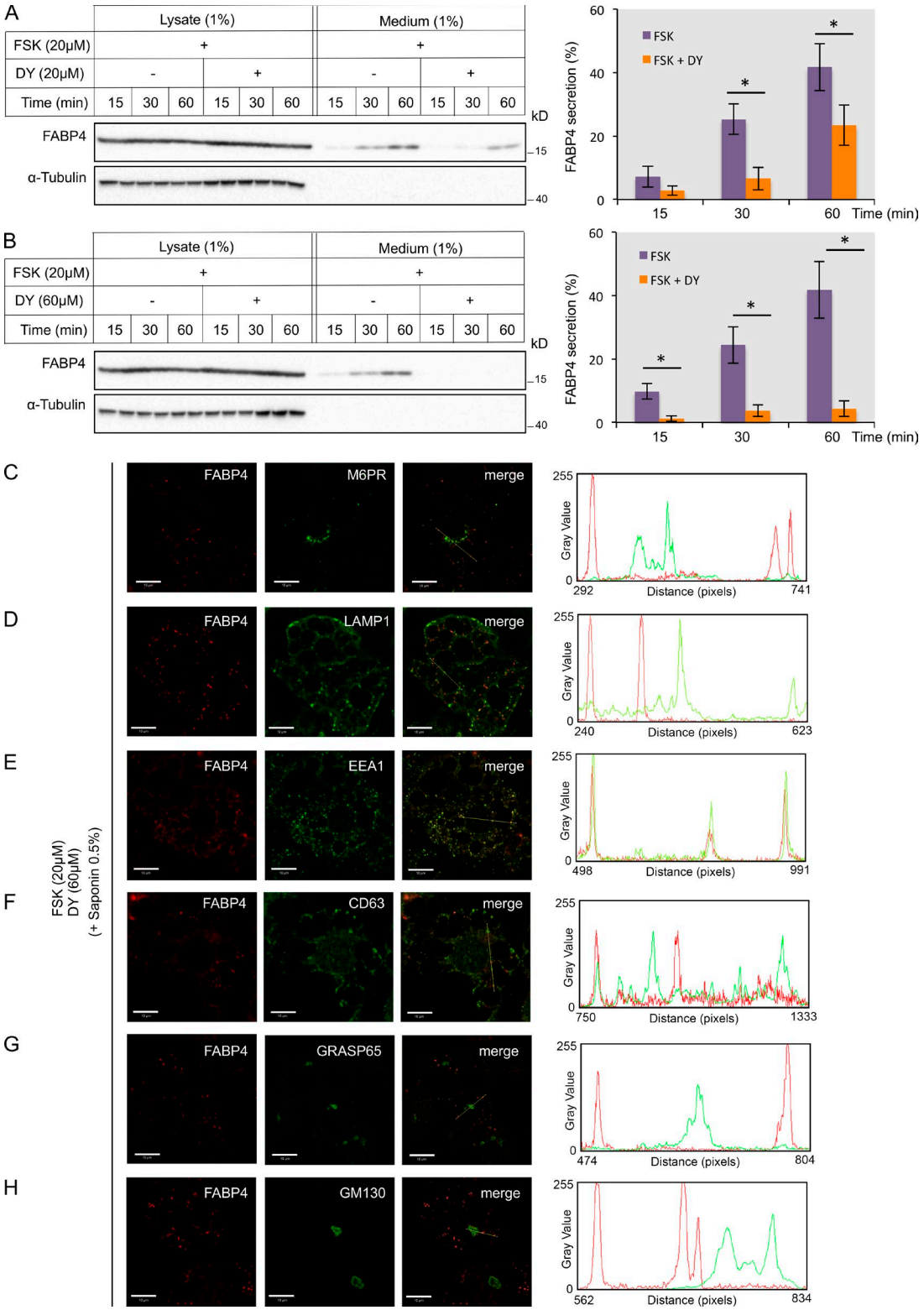

Figure 6. **Transport through the endocytic pathway is required for FABP4 secretion. (A and B)** Left: Adipocytes were incubated with 20 µM FSK in the presence or absence of 20 µM dynasore (A) or 60 µM dynasore (B), and at indicated times, medium fractions were collected and cells lysed. For each condition, performed in duplicate, 1% of total cell lysate and medium was analyzed by immunoblotting with anti-FABP4 and anti–α-tubulin antibodies. Right: Quantification of FABP4 secretion. For each condition, FABP4 secretion was calculated as a percentage of the signal detected in the medium compared with the total amount (the sum of FABP4 in both medium and lysate). Results are shown as the mean ± SD of three independent experiments. *, P < 0.05. **(C–H)** Left: Adipocytes were incubated in the presence of 20 µM FSK with 60 µM dynasore for 30 min, and cells were permeabilized with saponin before fixation. The colocalization of FABP4 with the indicated membrane markers was monitored by immunofluorescence microscopy. Bar, 10 µm. Pearson correlation coefficient (r) of colocalization, FABP4/M6PR r: 0.068 (C); FABP4/LAMP1 r: 0.079 (D); FABP4/EEA1 r: 0.427 (E); FABP4/CD63 r: 0.152 (F); FABP4/GRASP65 r: 0.029 (G); FABP4/GM130 r: 0.010 (H); *n* = 10 for each colocalization analysis. Right: Intensity profile graphs of FABP4 colocalization with the indicated membrane markers.

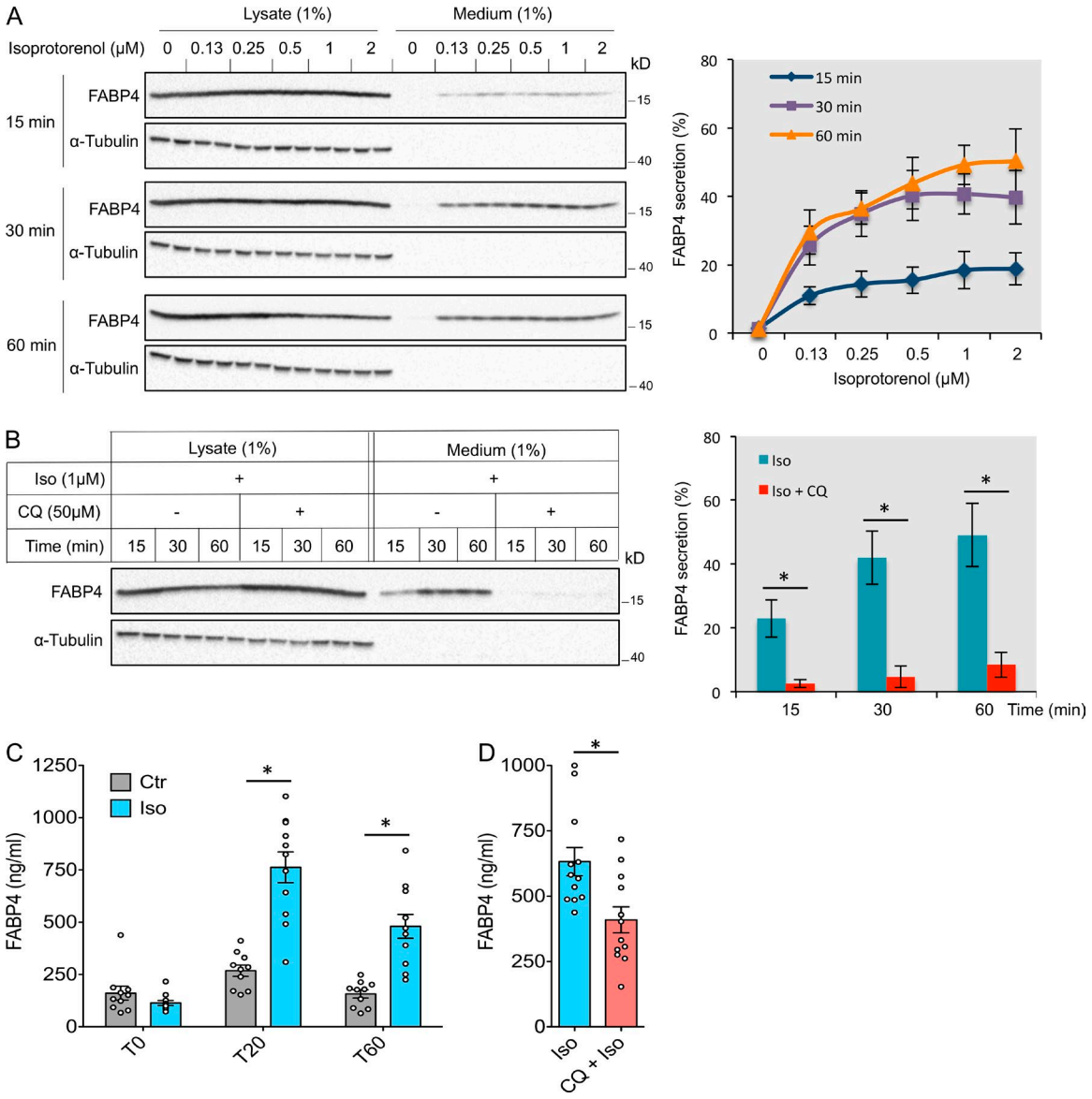

Figure 7. **CQ treatment inhibits FABP4 secretion in isoproterenol-treated mice. (A)** Left: Adipocytes were incubated with increasing concentrations of isoproterenol, and at indicated times, medium fractions were collected and cells lysed. For each condition, performed in duplicate, 1% of total cell lysate and medium was analyzed by immunoblotting with anti-FABP4 and anti–α-tubulin antibodies. Right: Quantification of FABP4 secretion. Results are shown as the mean ± SD of three independent experiments. **(B)** Left: Adipocytes were incubated with 1 μM isoproterenol in the presence or absence of 50 μM CQ, and at indicated times, medium fractions were collected and cells lysed. For each condition, performed in duplicate, 1% of total cell lysate and medium was analyzed by immunoblotting with anti-FABP4 and anti–α-tubulin antibodies. Right: Quantification of FABP4 secretion. Results are shown as the mean ± SD of three independent experiments. *, $P < 0.05$. **(A and B)** FABP4 secretion was calculated as a percentage of the signal detected in the medium compared with the total amount (the sum of FABP4 in both medium and lysate). **(C)** Plasma FABP4 levels in mice injected with saline (Ctr) or isoproterenol (Iso, 1 mg/kg). **(D)** Plasma FABP4 levels at T20 in mice preinjected with saline or CQ (50 mg/kg) 24 h and 1 h before isoproterenol injection (Iso, 1 mg/kg). Results in C and D are shown as the mean ± SEM. Twelve mice were used in each group. *, $P < 0.05$.

It is evident that lysosomes are not merely a compartment for degradation and recycling of organic material. Lysosomes also serve as platforms for metabolic sensing and signaling pathways (Sancak et al., 2010; Settembre et al., 2012; Settembre and Ballabio, 2014; Perera and Zoncu, 2016) and fuse with the plasma membrane to release their content into the extracellular space (Rodríguez et al., 1997, 1999; Andrews, 2000; Martinez et al., 2000; Jaiswal et al., 2002). But these studies do not reveal whether these diverse functions are performed by different populations of lysosomes and if so, what distinguishes one lysosome from another.

An acidic environment is required for the transport of protein toward lysosomes (Andrei et al., 1999), whereas an increase in lysosomal pH promotes lysosome exocytosis (Brown et al., 1985; Tapper and Sundler, 1990, 1995; Andrei et al., 1999). In line with these observations, it has recently been demonstrated that the position of lysosomes within the cell determines the luminal pH; peripheral lysosomes are less acidic compared with juxtanuclear lysosomes (Johnson et al., 2016). Thus, peripheral lysosomes might have reduced proteolytic activity. We propose that FABP4-containing endosomal membranes fuse with acidic lysosomes followed by their maturation to a higher luminal pH

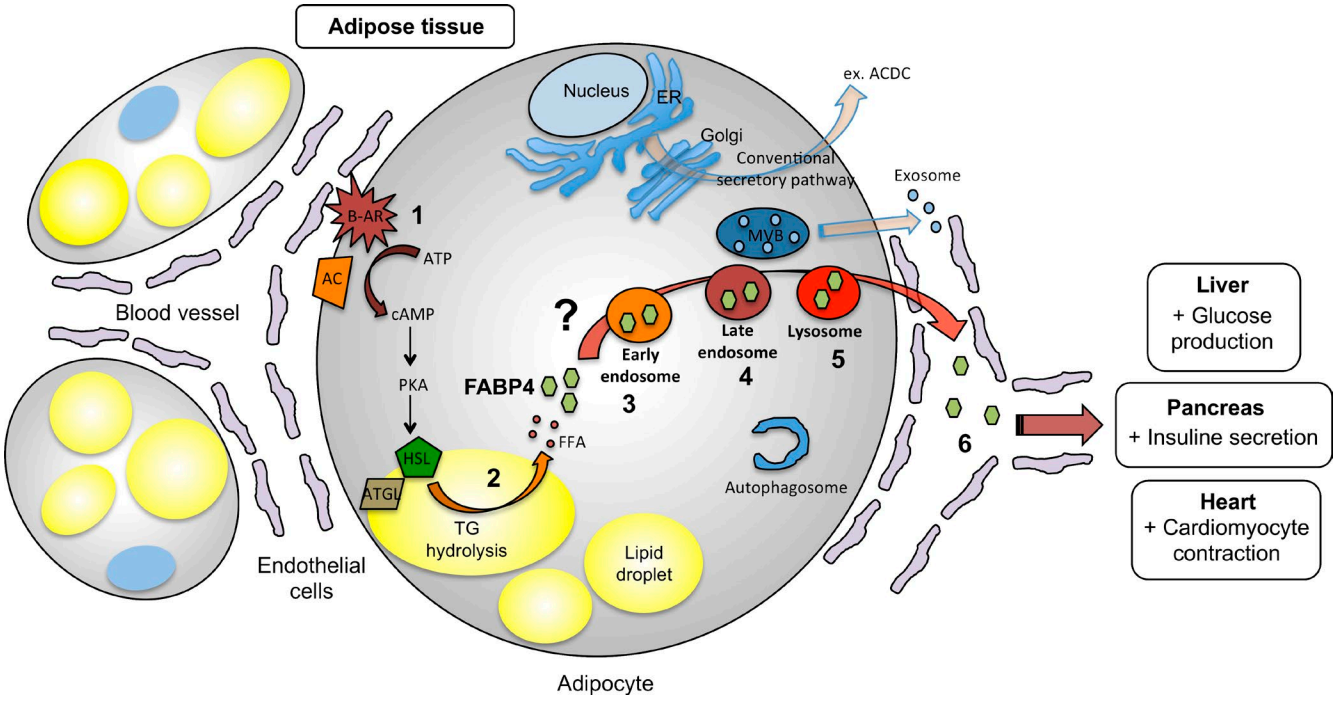

Figure 8. **Unconventional secretion of FABP4.** Schematic representation of the signaling and trafficking pathways required for FABP4 secretion in adipocytes. Upon lipolytic agonist stimulation (1), triglyceride hydrolysis (2) leads to FABP4 packaging in the endosomal/lysosomal compartment (3–5), followed by lysosome exocytosis and release of FABP4 to the extracellular space (6). Once circulating in the blood stream, FABP4 targets different cell types regulating essential biological functions such as the control of glucose production by hepatocytes, insulin secretion by pancreatic β-cells, or the control of cardiomyocyte contraction among others (Lamounier-Zepter et al., 2009; Cao et al., 2013; Girona et al., 2013; Wu et al., 2014; Hotamisligil and Bernlohr, 2015). AC, adenylate cyclase; ATGL, adipocyte triglyceride lipase; B-AR, β-adrenergic receptor; FFA, free fatty acid; HSL, hormone-sensitive lipase; TG, triglyceride.

and lower proteolytic activity; secretory lysosome movement to the cell periphery and subsequent fusion to the plasma membrane would thus result in FABP4 release.

Our findings that CQ administration reduces isoproterenol-mediated increase in plasma FABP4 secretion in mice suggest a means to manipulate its release. CQ is used for treating a large spectrum of diseases including malaria and autoimmune diseases such as rheumatoid arthritis and lupus erythematosus (Bernstein, 1991; Klinger et al., 2001; Savarino et al., 2003; Ben-Zvi et al., 2012; Thomé et al., 2013) and is beneficial in various complications associated with metabolic syndrome (Hodis et al., 1993; Bili et al., 2011; Cairoli et al., 2012; Hage et al., 2014). However, the favorable metabolic effects of CQ are ill-defined, and a better understanding of its mechanisms of action is needed to develop and to generalize its use. Our results offer a new and potentially beneficial use of CQ in treating metabolic syndrome. The evaluation of serum FABP4 in patients treated with CQ may provide encouragement for this avenue of therapy.

In conclusion, FABP4 is secreted by a process that involves endosomes and secretory lysosomes. This GRASP- and autophagy-independent secretory route for FABP4 release adds to the growing list of cytoplasmic proteins and pathways by which cells export cytoplasmic proteins (Nickel, 2010; Rabouille et al., 2012; Zhang and Schekman, 2013; Cruz-Garcia et al., 2014; Curwin et al., 2016). One way to look at these differences is to acknowledge the complexity and plasticity of the molecular machineries involved in membrane and protein trafficking, which is highly regulated in a cell type–dependent manner and linked to specific physiological or pathophysiological conditions. The alternative or most likely situation is that there are many different routes of collecting cytoplasmic proteins, but after this step, the cargoes are incorporated into an endosomal compartment and captured into intraluminal vesicles for exosome-mediated release, or the endosomes fuse with lysosomes, which fuse to the plasma membrane. A solution to these issues awaits a better molecular characterization of unconventional protein secretion.

Materials and methods

Reagents, antibodies, and plasmids

Reagents used in this study were obtained from the following sources. FSK, 1,9-ddFSK, IBMX, rosiglitazone, indomethacin, Clo, H89, isoproterenol, BFA, monensin, CQ, ammonium chloride, concanamycin A, wortmannin, dynasore, insulin, dexamethasone, DIDS, BSP, glibenclamide, and proteinase K were obtained from Sigma-Aldrich. Bafilomycin A1 was obtained from LC Laboratories. 3-Methyladenine was obtained from Cayman Chemical.

Antibodies used in this study were purchased from the following sources: Goat polyclonal antibody against FABP4, GRASP65, Rab7, and EEA1 were obtained from Santa Cruz Biotechnology. Rabbit polyclonal antibodies against FABP4, SytVII, and ACDC were purchased from Abcam. Rabbit polyclonal antibodies against Flag peptide, ERG IC53, LC3, and P62 (SQSTM1) were purchased from Sigma-Aldrich. Rabbit polyclonal antibodies against VAMP7 and GRASP55 were obtained from GeneTex and ProteinTech Group, respectively. Mouse monoclonal antibodies against α-tubulin (DM1A) and M6PR were obtained from Abcam. Rabbit polyclonal antibodies against CD63 and rat monoclonal antibody against LAMP1 were obtained from Santa Cruz Biotechnology. Mouse monoclonal antibodies against GM130, TSG101,

and transferrin receptor were obtained from BD, GeneTex, and Thermo Fisher Scientific, respectively. Mouse monoclonal antibodies against protein disulfide isomerase and Hrs were purchased from Enzo Life Sciences. We generated the rabbit polyclonal antibody against Sec22b as described previously (Schindler and Schekman, 2009). Secondary antibodies for immunofluorescence microscopy Alexa Fluor 488 or 568–conjugated donkey anti-rabbit, anti-mouse, anti-goat, and anti-rat were obtained from Thermo Fisher Scientific. Secondary antibodies for immunoblotting horseradish peroxidase–conjugated anti-mouse and anti-rabbit IgG were purchased from GE Healthcare, and horseradish peroxidase–conjugated anti-rat IgG was purchased from Sigma-Aldrich.

For lentiviral production, the transfer plasmid lentiCRISPRv2, the packaging plasmids pVSVg and psPAX2, and the plasmid encoding the Flag-tagged FABP4 were purchased from Addgene.

Cell culture, transfections, and treatments

The preadipose cell line 3T3-L1 was grown in complete medium consisting of DMEM containing 10% FBS, 100 U/ml penicillin, and 100 µg/ml streptomycin at 37°C with 5% CO_2. At confluence, complete medium was replaced by differentiation medium 1 containing DMEM, 10% FBS, 1 µg/ml insulin, 0.1 mM IBMX, 0.25 µM dexamethasone, and 2 µM rosiglitazone. After 48 h, differentiation medium 1 was replaced by differentiation medium 2 containing DMEM, 10% FBS, and 1 µg/ml insulin. After 48 h, differentiation medium 2 was replaced by complete medium, and 3T3-L1 cells differentiated into adipocytes were maintained in culture for 12 d.

For adipogenesis induction of MEF cells, primary MEF cells were isolated from embryos of wild-type C57BL/6N mice at day 13.5 of gestation. Embryos were isolated, and embryonic fibroblasts were prepared as described previously by trypsinization (Conner, 2001). Primary MEF cells were expanded in DMEM supplemented with 10% FBS, 100 U/ml penicillin, and 100 µg/ml streptomycin at 37°C with 5% CO_2 and maintained frozen in liquid nitrogen for further use. For differentiation to adipocytes, primary MEF cells were grown to reach confluence, and then complete medium was replaced by differentiation medium 1 containing DMEM, 10% FBS, 1 µg/ml insulin, 0.5 mM IBMX, 0.25 µM dexamethasone, and 10 µM indomethacin. After 72 h, differentiation medium 1 was replaced by differentiation medium 2 containing DMEM, 10% FBS, and 1 µg/ml insulin, and MEF cells differentiated into adipocytes were maintained in culture for 12 d by replacing medium every 2 d.

Control MEF cells and Atg5 knockout MEF cells were provided by N. Mizushima (Tokyo Medical and Dental University, Japan; Kuma et al., 2004). In brief, control MEF cells and Atg5 knockout MEF cells were isolated from embryos of C57BL/6N mice at day 13.5 of gestation and immortalized after transformation with pEF321-T, an SV40 large T antigen expression vector. Adipocytes, MEF, HEK293T, and PC-3 cells were grown in complete medium at 37°C with 5% CO_2.

We preincubated adipocytes for 20 min at the indicated concentrations for treatment with BFA, monensin, wortmannin, 3-methyladenin, Clo, H89, CQ, ammonium chloride, bafilomycin A1, concanamycin A, DIDS, BSP, and glibenclamide. Then cells were washed three times with complete medium and incubated for the indicated times in complete medium with lipolytic agonist (FSK, IBMX, or isoproterenol) and the indicated agents. For analysis using MEF cells, FABP4 secretion was induced by incubating cells in starvation conditions using EBSS.

Plasmids were transfected in MEF and HEK293T cells with Lipofectamine 2000 (Invitrogen) following the manufacturer's recommendations.

Lentivirus production and adipocyte transduction

The plasmid LentiCRISPRv2 with single guide RNA (sgRNA) was cloned using the oligos indicated in Table S1. For each targeted gene, the pair of oligos was annealed and cloned in the LentiCRISPRv2 vector digested with BsmBI. The plasmid LentiCRISPRv2 (10 µg) carrying specific sgRNA was then transfected using Lipofectamine 2000 (Invitrogen) following the manufacturer's recommendations into HEK293T cells at 50% confluence the day of transfection along with lentiviral packaging plasmids pVSVg (3.5 µg) and psPAX2 (6.5 µg; Addgene). Transfection was performed for each sgRNA using one 10-cm dish. After a 24-h transfection, the medium was changed, and after an additional 24 h, the medium was removed and filtered through a 0.45-µm low-protein binding membrane (VWR International). Adipocytes were then transduced with the virus via spinfection. In brief, adipocytes at T1 after differentiation, plated in 6-well plates, were incubated with 3 ml per well of lentivirus particles supplemented with 8 µg/ml polybrene (Sigma-Aldrich). The 6-well plates were then centrifuged at 900 *g* for 45 min at 37°C. After 24 h, medium was replaced with fresh medium, and after additional 24 h, 2 µg/ml puromycin (Sigma-Aldrich) was added to select transduced cells. After an additional 7 d, adipocytes at T9 after differentiation were subjected to lipolytic agonist stimulation and drug treatment.

Immunoblot

Cells were ruptured in lysis buffer (50 mM Tris, pH 7.4, 150 mM NaCl, 0.1% SDS, 1% [vol/vol] Triton X-100, and 0.5% sodium deoxycholate) supplemented with protease inhibitors (Sigma-Aldrich), 1 mM Na_3VO_4, and 25 mM sodium fluoride and centrifuged at 16,000 *g* for 15 min. Media were harvested and centrifuged first at 1,000 *g* for 10 min followed by a centrifugation at 16,000 *g* for 15 min. For adipocyte experimentation, 1% of total cell lysate and media fractions were subjected to immunoblotting. For MEF cells experiments, 3% of total cell lysate and 18% of total medium fractions were concentrated using 55% TCA, and protein precipitates were subjected to SDS-PAGE and then immunoblot analysis. For medium samples concentrated by TCA protein precipitation, 30 µg of bovine serum albumin and 150 µl of 55% TCA were added to 1 ml of medium and incubated 30 min on ice. Medium was then centrifuged at 16,000 *g* for 30 min at 4°C and supernatant removed. After another centrifugation at 16,000 *g* for 1 min at 4°C, the precipitated pellet fraction was dried and resuspended in 1× SDS sample buffer. Samples were incubated with 1× SDS sample buffer at 95°C for 5 min and loaded onto 4–20% criterion precast gels (Bio-Rad). Proteins were blotted onto a nitrocellulose membrane, blocked with 5% bovine serum albumin, and probed with primary antibody overnight. Membranes were then washed and incubated with the corresponding secondary antibody. Signals were acquired with a Chemidoc MP Imaging System (Bio-Rad), and ImageJ (National Institutes of Health) was used for quantification.

Extracellular vesicle analysis

Adipocytes were incubated in complete medium in the presence of FSK for 4 h. DMEM medium used was precentrifuged 18 h at 100,000 *g* (SW 28 Ti rotor; Beckman) at 4°C to remove extracellular vesicles. Medium was harvested and first centrifuged at 600 *g* for 10 min to remove detached cells. Then, the cleared medium was subjected to sequential differentiation at 1,000 *g* (10 min), 15,000 *g* (20 min), and 100,000 *g* (60 min, TLA100.3 rotor; Beckman) to collect the sedimented membranes at each step, which were suspended in lysis buffer. After the last centrifugation, the supernantant solution was collected and used as a soluble fraction.

Cytosol and total membrane preparation

Adipocytes were incubated in the presence or absence of FSK with or without CQ for 1 h. Cells were then washed three times with PBS, harvested by scraping, centrifuged at 600 *g* for 5 min, and homogenized by passing through a 22G needle in a 1.5× cell pellet volume of B88 buffer (20 mM Hepes-KOH, pH 7.2, 250 mM sorbitol, 150 mM potassium

acetate, and 5 mM magnesium acetate) plus cocktail protease inhibitors (Sigma-Aldrich). The cell homogenates were first centrifuged at 1,000 *g* for 10 min to remove unbroken cells and nuclei and then at 100,000 *g* for 1 h to collect total membranes. Supernatant solutions were collected and used as cytosolic fractions. Membrane pellets were washed in B88 and subjected to another centrifugation at 100,000 *g* for 1 h. Finally, the total membranes were suspended in lysis buffer in the same volume as the corresponding cytosolic fraction.

Membrane flotation assay

Adipocytes were incubated in the presence of FSK and CQ, and total membrane fractions were collected as described in the previous paragraph. Total membranes were suspended in 0.3 ml B88 buffer containing 60% (wt/vol) Nycodenz (Accurate Chemical) and overlaid with 0.6 ml B88 containing 40% Nycodenz and 0.1 ml B88. The Nycodenz gradient was centrifuged at 250,000 *g* for 90 min (TLS 55 rotor; Beckman), and subsequently 10 fractions, 0.1 ml each, were collected from the top and analyzed by immunoblot for the indicated markers.

Protease treatment

Adipocytes were incubated in the presence of FSK and CQ, and total membrane fractions were collected as described in the Cytosol and total membrane preparation section. Total membranes were suspended in B88 buffer and incubated with increasing concentrations of proteinase K in the presence or absence of 0.5% Triton X-100 for 30 min on ice, after which 1 mM PMSF was added to the reaction and incubated 15 min on ice before the addition of loading buffer.

Three-step membrane fractionation

Adipocytes (twelve 15-cm dishes for each condition) were incubated in the presence or absence of FSK with or without CQ for 1 h. Cells were washed three times with PBS, harvested by scraping, centrifuged at 600 *g* for 5 min, and homogenized by passing through a 22-G needle in a 1.5× cell pellet volume of buffer containing 20 mM Hepes-KOH, pH 7.2, 400 mM sucrose, and 1 mM EDTA. The cells homogenates were first centrifuged at 1,000 *g* for 10 min to remove unbroken cells and nuclei and then subjected to sequential centrifugation at 3,000 *g* (10 min), 25,000 *g*, (20 min) and 100,000 *g* (30 min, TLA100.3 rotor) to collect the sedimented membranes at each step. After the last centrifugation, supernatant solutions were collected and used as cytosolic fractions. The 25,000 *g* membrane pellet, which contained the highest FABP4 signal when adipocytes were incubated in the presence of FSK and CQ, was suspended in 0.75 ml of 1.25 M sucrose buffer and overlaid with 0.5 ml of 1.1 M and 0.5 ml of 0.25 M sucrose buffer (Golgi isolation kit; Sigma-Aldrich). Centrifugation was performed at 120,000 *g* for 2 h (TLS 55 rotor; Beckman), after which two fractions, one at the interface between 0.25 and 1.1 M sucrose (light fraction) and the pellet fraction on the bottom (P fraction), were separated. The presence of FABP4 in the two fractions was then evaluated, and the light fraction was selected and suspended in 1 ml 19% OptiPrep for a step gradient containing 0.5 ml 22.5%, 1 ml 19% (sample), 0.9 ml 16%, 0.9 ml 12%, 1 ml 8%, 0.5 ml 5%, and 0.2 ml 0% OptiPrep each. Each density of OptiPrep was prepared by diluting 50% OptiPrep (20 mM Tricine-KOH, pH 7.4, 42 mM sucrose, and 1 mM EDTA) with a buffer containing 20 mM Tricine-KOH, pH 7.4, 250 mM sucrose, and 1 mM EDTA. The OptiPrep gradient was centrifuged at 150,000 *g* for 3 h (SW 55 Ti rotor; Beckman), and subsequently 10 fractions, 0.5 ml each, were collected from the top. Fractions were diluted with B88 buffer, and membranes were collected by centrifugation at 100,000 *g* for 1 h. Each membrane fraction was normalized for the content of PC and evaluated by immunoblot for the presence of FABP4 and markers of specific membrane compartments. The PC content in each fraction was measured using the Phosphatidylcholine Colorimetric/Fluorometric Assay kit (BioVision) following the manufacturer's recommendations.

Immunofluorescence microscopy

Cells grown on coverslips were fixed with 4% paraformaldehyde in PBS for 10 min followed by permeabilization with 0.1% Triton X100 at room temperature and incubation with blocking buffer (2.5% FCS and 0.1% Triton X-100 in PBS) for 30 min at room temperature. Cells were then incubated with primary antibody followed by a PBS wash and incubated with secondary antibody (donkey anti-mouse, anti-rabbit, anti-goat, or anti-rat Alexa Fluor 488 or 568). DAPI was used to stain the DNA. For FABP4 localization studies in permeabilized cells, adipocytes were washed twice with room temperature KHM buffer (125 mM potassium acetate, 25 mM Hepes, pH 7.2, and 2.5 mM magnesium acetate). Cells were then permeabilized by incubation in KHM buffer containing 0.1% saponin for 5 min on ice followed by a wash for 5 min at room temperature with KHM buffer. Cells were subsequently fixed with 4% paraformaldehyde and processed for immunofluorescence microscopy. Images were acquired using Zen 2010 Software on an LSM 710 confocal microscope system (ZEISS) with a Plan Apochromat 63× 1.4 numerical aperture objective. For SIM analysis, FABP4 and LAMP1 localization images in Fig. 5 D were taken with an Elyra PS.1 (ZEISS) in SIM mode with a Plan Apochromat 100× 1.47 numerical aperture objective. SIM images were processed using Zen 2012 black imaging software. Colocalization quantifications were performed using the Costes method of thresholding with object Pearson's analysis using Imaris 8.2.0 by Bitplane AG. Intensity profile graphs of the confocal images were calculated by a pixel-based method by ImageJ.

For neutral lipid staining of adipocytes, we fixed cells with 4% paraformaldehyde in PBS for 10 min followed by labeling with LipidTOX Deep Red neutral lipid stain (Thermo Fisher Scientific) following the manufacturer's recommendations.

Surface LAMP1 analysis

Adipocytes were incubated in the presence or absence of 20 µM FSK for 2 h and then washed three times with PBS. For flow cytometry analysis, adipocytes were detached after incubation with 0.5 mM EDTA for 10 min and cells fixed with 1% paraformaldehyde in PBS for 10 min. For immunofluorescence microscopy, cells were fixed with 4% paraformaldehyde in PBS for 10 min. After fixation, adipocytes were incubated with blocking buffer (2.5% FCS in PBS) for 30 min at room temperature and then incubated with the rat monoclonal antibody against the luminal domain of LAMP1 (LAMP1-1DB4; Santa Cruz Biotechnology). After a 45-min incubation, cells were washed and incubated with Alexa Fluor 488–conjugated anti-rat secondary antibody. Finally, adipocytes were analyzed on a confocal microscope as described in the Immunofluorescence microscopy section or on a LSR Fortessa flow cytometer (BD Biosciences).

Treatment of mice

Male C57BL/6J mice (Charles River) were housed in a temperature-controlled pathogen-free environment (transgenic animal housing of Bordeaux University) with a 12-h light/dark cycle and given free access to food and water. The study followed guidelines of the animal research ethical committee of Aquitaine Poitou-Charentes. Isoproterenol (1 mg/kg, diluted in saline) was administered by intraperitoneal injection. Control mice received an identical amount of vehicle. For CQ treatment, CQ (50 mg/kg, diluted in saline) was administered by intraperitoneal injection 24 and 1 h before isoproterenol injection. Control mice received an identical amount of vehicle. Blood samples were collected by tail bleeding in the presence of 10 mM EDTA immediately

after isoproterenol injection and 20 and 60 min after isoproterenol injection. Blood samples were centrifuged at 1,000 *g* for 15 min, plasma was collected, and the FABP4 concentration was determined by ELI SA using a mouse adipocyte fatty acid–binding protein (FABP4) ELISA kit from BioVendor.

Statistical analysis

Data are presented as mean ± SD. Differences in the mean values between two groups were assessed by a two-tailed Student's *t* test. *, $P < 0.05$ was taken to imply statistical significance.

Online supplemental material

Fig. S1 shows that FABP4 is highly expressed and secreted once 3T3-L1 and MEF cells are differentiated into adipocytes. Fig. S2 shows that ERGIC dispersal as well as GRASP55 and GRASP65 deletion do not affect FABP4 secretion. Fig. S3 shows that FABP4 secretion is inhibited by CQ, concanamycin A, and bafilomycin A1. Fig. S4 shows that FABP4 secretion is not impaired by ABC transport inhibitors. Fig. S5 shows that in FSK- and CQ treated-cells, FABP4 does not colocalize with Golgi and early endosome markers. Table S1 shows the pairs of oligonucleotides cloned in the plasmid LentiCRISPRv2 to target specific genes with sgRNA. A supplemental PDF showing replicate datasets for the experiments shown in Fig. 1 A; Fig. 2, C, E, and H; Fig. 3, A, B, E, and F; Fig. 6, A and B; Fig. S2 D; Fig. S3, B and C; and Fig. S4 B is also included.

Acknowledgments

We thank members of the Malhotra laboratory and Schekman laboratory for helpful discussion. We thank B. Lesch, A. Fisher, A. Killilea, C. Tasto, and D. Schichnes for technical assistance.

J. Villeneuve acknowledges support from a Marie Curie International Outgoing Fellowship within the European community Seventh Framework Programme. R. Schekman is supported as an investigator of the Howard Hughes Medical Institute and a Senior Fellow of the University of California, Berkeley, Miller Institute. Research reported in this publication was supported in part by the National Institutes of Health S10 program under grants 1S10RR026866-01 and 1S10OD018136-01. We acknowledge support from the Spanish Ministry of Economy and Competitiveness through the Program Centro de Excelencia Severo Ochoa 2013–2017 (grant SEV-2012-0208) and support from the Centres de Recerca de Catalunya (CERCA) Program/Generalitat de Catalunya. V. Malhotra is an Institució Catalana de Recerca i Estudis Avançats professor at the Center for Genomic Regulation, and the work in his laboratory is funded by grants from the Ministry of Economy and Competitiveness' Plan Nacional (BFU2013-44188-P), Consolider (CSD2009-00016), and the European Research Council (268692). The project has received research funding from the European Union. This paper reflects only the authors' views. The National Institutes of Health and the European Union are not liable for any use that may be made of the information contained therein.

The authors declare no competing financial interests.

Author contributions: J. Villeneuve, J. Ripoche, V. Malhotra, and R. Schekman conceptualized the experiments. J. Villeneuve performed and analyzed most of the experiments, with contributions from L. Bassaganyas, S. Lepreux, M. Chiritoiu, and P. Costet. J. Villeneuve, V. Malhotra, and R. Schekman wrote the original and revised manuscripts with contributions from the other authors.

Submitted: 11 May 2017
Revised: 9 October 2017
Accepted: 14 November 2017

References

Andrei, C., C. Dazzi, L. Lotti, M.R. Torrisi, G. Chimini, and A. Rubartelli. 1999. The secretory route of the leaderless protein interleukin 1beta involves exocytosis of endolysosome-related vesicles. *Mol. Biol. Cell.* 10:1463–1475. https://doi.org/10.1091/mbc.10.5.1463

Andrews, N.W. 2000. Regulated secretion of conventional lysosomes. *Trends Cell Biol.* 10:316–321. https://doi.org/10.1016/S0962-8924(00)01794-3

Ben-Zvi, I., S. Kivity, P. Langevitz, and Y. Shoenfeld. 2012. Hydroxychloroquine: from malaria to autoimmunity. *Clin. Rev. Allergy Immunol.* 42:145–153. https://doi.org/10.1007/s12016-010-8243-x

Bernstein, H.N. 1991. Ocular safety of hydroxychloroquine. *Ann. Ophthalmol.* 23:292–296.

Bili, A., J.A. Sartorius, H.L. Kirchner, S.J. Morris, L.J. Ledwich, J.L. Antohe, S. Dancea, E.D. Newman, and M.C. Wasko. 2011. Hydroxychloroquine use and decreased risk of diabetes in rheumatoid arthritis patients. *J. Clin. Rheumatol.* 17:115–120. https://doi.org/10.1097/RHU.0b013e318214b6b5

Bowman, E.J., A. Siebers, and K. Altendorf. 1988. Bafilomycins: a class of inhibitors of membrane ATPases from microorganisms, animal cells, and plant cells. *Proc. Natl. Acad. Sci. USA.* 85:7972–7976. https://doi.org/10.1073/pnas.85.21.7972

Brown, J.A., E.K. Novak, and R.T. Swank. 1985. Effects of ammonia on processing and secretion of precursor and mature lysosomal enzyme from macrophages of normal and pale ear mice: evidence for two distinct pathways. *J. Cell Biol.* 100:1894–1904. https://doi.org/10.1083/jcb.100.6.1894

Bruns, C., J.M. McCaffery, A.J. Curwin, J.M. Duran, and V. Malhotra. 2011. Biogenesis of a novel compartment for autophagosome-mediated unconventional protein secretion. *J. Cell Biol.* 195:979–992. https://doi.org/10.1083/jcb.201106098

Burak, M.F., K.E. Inouye, A. White, A. Lee, G. Tuncman, E.S. Calay, M. Sekiya, A. Tirosh, K. Eguchi, G. Birrane, et al. 2015. Development of a therapeutic monoclonal antibody that targets secreted fatty acid-binding protein aP2 to treat type 2 diabetes. *Sci. Transl. Med.* 7:319ra205. https://doi.org/10.1126/scitranslmed.aac6336

Cairoli, E., M. Rebella, N. Danese, V. Garra, and E.F. Borba. 2012. Hydroxychloroquine reduces low-density lipoprotein cholesterol levels in systemic lupus erythematosus: a longitudinal evaluation of the lipid-lowering effect. *Lupus.* 21:1178–1182. https://doi.org/10.1177/0961203312450084

Cao, H., M. Sekiya, M.E. Ertunc, M.F. Burak, J.R. Mayers, A. White, K. Inouye, L.M. Rickey, B.C. Ercal, M. Furuhashi, et al. 2013. Adipocyte lipid chaperone AP2 is a secreted adipokine regulating hepatic glucose production. *Cell Metab.* 17:768–778. https://doi.org/10.1016/j.cmet.2013.04.012

Cong, L., F.A. Ran, D. Cox, S. Lin, R. Barretto, N. Habib, P.D. Hsu, X. Wu, W. Jiang, L.A. Marraffini, and F. Zhang. 2013. Multiplex genome engineering using CRISPR/Cas systems. *Science.* 339:819–823. https://doi.org/10.1126/science.1231143

Conner, D.A. 2001. Mouse embryo fibroblast (MEF) feeder cell preparation. Curr. Protoc. Mol. Biol. Chapter 23:Unit 23 22.

Cruz-Garcia, D., A.J. Curwin, J.F. Popoff, C. Bruns, J.M. Duran, and V. Malhotra. 2014. Remodeling of secretory compartments creates CUPS during nutrient starvation. *J. Cell Biol.* 207:695–703. https://doi.org/10.1083/jcb.201407119

Cruz-Garcia, D., N. Brouwers, J.M. Duran, G. Mora, A.J. Curwin, and V. Malhotra. 2017. A diacidic motif determines unconventional secretion of wild-type and ALS-linked mutant SOD1. *J. Cell Biol.* 216:2691–2700

Curwin, A.J., N. Brouwers, M. Alonso Y Adell, D. Teis, G. Turacchio, S. Parashuraman, P. Ronchi, and V. Malhotra. 2016. ESCRT-III drives the final stages of CUPS maturation for unconventional protein secretion. *eLife.* 5:5. https://doi.org/10.7554/eLife.16299

Dupont, N., S. Jiang, M. Pilli, W. Ornatowski, D. Bhattacharya, and V. Deretic. 2011. Autophagy-based unconventional secretory pathway for extracellular delivery of IL-1β. *EMBO J.* 30:4701–4711. https://doi.org/10.1038/emboj.2011.398

Duran, J.M., C. Anjard, C. Stefan, W.F. Loomis, and V. Malhotra. 2010. Unconventional secretion of Acb1 is mediated by autophagosomes. *J. Cell Biol.* 188:527–536. https://doi.org/10.1083/jcb.200911154

Ertunc, M.E., J. Sikkeland, F. Fenaroli, G. Griffiths, M.P. Daniels, H. Cao, F. Saatcioglu, and G.S. Hotamisligil. 2015. Secretion of fatty acid binding protein aP2 from adipocytes through a nonclassical pathway in response to adipocyte lipase activity. *J. Lipid Res.* 56:423–434. https://doi.org/10.1194/jlr.M055798

Ge, L., D. Melville, M. Zhang, and R. Schekman. 2013. The ER-Golgi intermediate compartment is a key membrane source for the LC3

lipidation step of autophagosome biogenesis. *eLife.* 2:e00947. https://doi.org/10.7554/eLife.00947

Girona, J., R. Rosales, N. Plana, P. Saavedra, L. Masana, and J.C. Vallvé. 2013. FABP4 induces vascular smooth muscle cell proliferation and migration through a MAPK-dependent pathway. *PLoS One.* 8:e81914. https://doi.org/10.1371/journal.pone.0081914

Giuliani, F., A. Grieve, and C. Rabouille. 2011. Unconventional secretion: a stress on GRASP. *Curr. Opin. Cell Biol.* 23:498–504. https://doi.org/10.1016/j.ceb.2011.04.005

Gregor, M.F., and G.S. Hotamisligil. 2011. Inflammatory mechanisms in obesity. *Annu. Rev. Immunol.* 29:415–445. https://doi.org/10.1146/annurev-immunol-031210-101322

Hage, M.P., M.R. Al-Badri, and S.T. Azar. 2014. A favorable effect of hydroxychloroquine on glucose and lipid metabolism beyond its anti-inflammatory role. *Ther. Adv. Endocrinol. Metab.* 5:77–85. https://doi.org/10.1177/2042018814547204

Hodis, H.N., F.P. Quismorio Jr., E. Wickham, and D.H. Blankenhorn. 1993. The lipid, lipoprotein, and apolipoprotein effects of hydroxychloroquine in patients with systemic lupus erythematosus. *J. Rheumatol.* 20:661–665.

Hotamisligil, G.S., and D.A. Bernlohr. 2015. Metabolic functions of FABPs--mechanisms and therapeutic implications. *Nat. Rev. Endocrinol.* 11:592–605. https://doi.org/10.1038/nrendo.2015.122

Jaiswal, J.K., N.W. Andrews, and S.M. Simon. 2002. Membrane proximal lysosomes are the major vesicles responsible for calcium-dependent exocytosis in nonsecretory cells. *J. Cell Biol.* 159:625–635. https://doi.org/10.1083/jcb.200208154

Johnson, D.E., P. Ostrowski, V. Jaumouillé, and S. Grinstein. 2016. The position of lysosomes within the cell determines their luminal pH. *J. Cell Biol.* 212:677–692. https://doi.org/10.1083/jcb.201507112

Kataoka, T., K. Takaku, J. Magae, N. Shinohara, H. Takayama, S. Kondo, and K. Nagai. 1994. Acidification is essential for maintaining the structure and function of lytic granules of CTL: Effect of concanamycin A, an inhibitor of vacuolar type H(+)-ATPase, on CTL-mediated cytotoxicity. *J. Immunol.* 153:3938–3947.

Kinseth, M.A., C. Anjard, D. Fuller, G. Guizzunti, W.F. Loomis, and V. Malhotra. 2007. The Golgi-associated protein GRASP is required for unconventional protein secretion during development. *Cell.* 130:524–534. https://doi.org/10.1016/j.cell.2007.06.029

Klinger, G., Y. Morad, C.A. Westall, C. Laskin, K.A. Spitzer, G. Koren, S. Ito, and R.J. Buncic. 2001. Ocular toxicity and antenatal exposure to chloroquine or hydroxychloroquine for rheumatic diseases. *Lancet.* 358:813–814. https://doi.org/10.1016/S0140-6736(01)06004-4

Klionsky, D.J., F.C. Abdalla, H. Abeliovich, R.T. Abraham, A. Acevedo-Arozena, K. Adeli, L. Agholme, M. Agnello, P. Agostinis, J.A. Aguirre-Ghiso, et al. 2012. Guidelines for the use and interpretation of assays for monitoring autophagy. *Autophagy.* 8:445–544. https://doi.org/10.4161/auto.19496

Kralisch, S., T. Ebert, U. Lossner, B. Jessnitzer, M. Stumvoll, and M. Fasshauer. 2014. Adipocyte fatty acid-binding protein is released from adipocytes by a non-conventional mechanism. *Int. J. Obes.* 38:1251–1254. https://doi.org/10.1038/ijo.2013.232

Kralisch, S., N. Klöting, T. Ebert, M. Kern, A. Hoffmann, K. Krause, B. Jessnitzer, U. Lossner, I. Sommerer, M. Stumvoll, and M. Fasshauer. 2015. Circulating adipocyte fatty acid-binding protein induces insulin resistance in mice in vivo. *Obesity (Silver Spring).* 23:1007–1013. https://doi.org/10.1002/oby.21057

Kuma, A., M. Hatano, M. Matsui, A. Yamamoto, H. Nakaya, T. Yoshimori, Y. Ohsumi, T. Tokuhisa, and N. Mizushima. 2004. The role of autophagy during the early neonatal starvation period. *Nature.* 432:1032–1036. https://doi.org/10.1038/nature03029

Lamounier-Zepter, V., C. Look, J. Alvarez, T. Christ, U. Ravens, W.H. Schunck, M. Ehrhart-Bornstein, S.R. Bornstein, and I. Morano. 2009. Adipocyte fatty acid-binding protein suppresses cardiomyocyte contraction: a new link between obesity and heart disease. *Circ. Res.* 105:326–334. https://doi.org/10.1161/CIRCRESAHA.109.200501

Lee, M.C., E.A. Miller, J. Goldberg, L. Orci, and R. Schekman. 2004. Bi-directional protein transport between the ER and Golgi. *Annu. Rev. Cell Dev. Biol.* 20:87–123. https://doi.org/10.1146/annurev.cellbio.20.010403.105307

Levi, S.K., and B.S. Glick. 2007. GRASPing unconventional secretion. *Cell.* 130:407–409. https://doi.org/10.1016/j.cell.2007.07.030

Ling, H., P. Ardjomand, S. Samvakas, A. Simm, G.L. Busch, F. Lang, K. Sebekova, and A. Heidland. 1998. Mesangial cell hypertrophy induced by NH4Cl: role of depressed activities of cathepsins due to elevated lysosomal pH. *Kidney Int.* 53:1706–1712. https://doi.org/10.1046/j.1523-1755.1998.00952.x

Luo, D.X., M.C. Huang, J. Ma, Z. Gao, D.F. Liao, and D. Cao. 2011. Aldo-keto reductase family 1, member B10 is secreted through a lysosome-mediated non-classical pathway. *Biochem. J.* 438:71–80. https://doi.org/10.1042/BJ20110111

Macia, E., M. Ehrlich, R. Massol, E. Boucrot, C. Brunner, and T. Kirchhausen. 2006. Dynasore, a cell-permeable inhibitor of dynamin. *Dev. Cell.* 10:839–850. https://doi.org/10.1016/j.devcel.2006.04.002

Malhotra, V. 2013. Unconventional protein secretion: an evolving mechanism. *EMBO J.* 32:1660–1664. https://doi.org/10.1038/emboj.2013.104

Mali, P., L. Yang, K.M. Esvelt, J. Aach, M. Guell, J.E. DiCarlo, J.E. Norville, and G.M. Church. 2013. RNA-guided human genome engineering via Cas9. *Science.* 339:823–826. https://doi.org/10.1126/science.1232033

Mambula, S.S., and S.K. Calderwood. 2006. Heat shock protein 70 is secreted from tumor cells by a nonclassical pathway involving lysosomal endosomes. *J. Immunol.* 177:7849–7857. https://doi.org/10.4049/jimmunol.177.11.7849

Manjithaya, R., C. Anjard, W.F. Loomis, and S. Subramani. 2010. Unconventional secretion of *Pichia pastoris* Acb1 is dependent on GRASP protein, peroxisomal functions, and autophagosome formation. *J. Cell Biol.* 188:537–546. https://doi.org/10.1083/jcb.200911149

Marsh, M., and H.T. McMahon. 1999. The structural era of endocytosis. *Science.* 285:215–220. https://doi.org/10.1126/science.285.5425.215

Martinez, I., S. Chakrabarti, T. Hellevik, J. Morehead, K. Fowler, and N.W. Andrews. 2000. Synaptotagmin VII regulates Ca(2+)-dependent exocytosis of lysosomes in fibroblasts. *J. Cell Biol.* 148:1141–1149. https://doi.org/10.1083/jcb.148.6.1141

Mita, T., M. Furuhashi, S. Hiramitsu, J. Ishii, K. Hoshina, S. Ishimura, T. Fuseya, Y. Watanabe, M. Tanaka, K. Ohno, et al. 2015. FABP4 is secreted from adipocytes by adenyl cyclase-PKA- and guanylyl cyclase-PKG-dependent lipolytic mechanisms. *Obesity (Silver Spring).* 23:359–367. https://doi.org/10.1002/oby.20954

Mizushima, N., A. Yamamoto, M. Hatano, Y. Kobayashi, Y. Kabeya, K. Suzuki, T. Tokuhisa, Y. Ohsumi, and T. Yoshimori. 2001. Dissection of autophagosome formation using Apg5-deficient mouse embryonic stem cells. *J. Cell Biol.* 152:657–668. https://doi.org/10.1083/jcb.152.4.657

Nickel, W. 2010. Pathways of unconventional protein secretion. *Curr. Opin. Biotechnol.* 21:621–626. https://doi.org/10.1016/j.copbio.2010.06.004

Nickel, W., and C. Rabouille. 2009. Mechanisms of regulated unconventional protein secretion. *Nat. Rev. Mol. Cell Biol.* 10:148–155. https://doi.org/10.1038/nrm2617

Nicoziani, P., F. Vilhardt, A. Llorente, L. Hilout, P.J. Courtoy, K. Sandvig, and B. van Deurs. 2000. Role for dynamin in late endosome dynamics and trafficking of the cation-independent mannose 6-phosphate receptor. *Mol. Biol. Cell.* 11:481–495. https://doi.org/10.1091/mbc.11.2.481

Perera, R.M., and R. Zoncu. 2016. The Lysosome as a Regulatory Hub. *Annu. Rev. Cell Dev. Biol.* 32:223–253. https://doi.org/10.1146/annurev-cellbio-111315-125125

Praefcke, G.J., and H.T. McMahon. 2004. The dynamin superfamily: universal membrane tubulation and fission molecules? *Nat. Rev. Mol. Cell Biol.* 5:133–147. https://doi.org/10.1038/nrm1313

Rabouille, C., V. Malhotra, and W. Nickel. 2012. Diversity in unconventional protein secretion. *J. Cell Sci.* 125:5251–5255. https://doi.org/10.1242/jcs.103630

Rao, S.K., C. Huynh, V. Proux-Gillardeaux, T. Galli, and N.W. Andrews. 2004. Identification of SNAREs involved in synaptotagmin VII-regulated lysosomal exocytosis. *J. Biol. Chem.* 279:20471–20479. https://doi.org/10.1074/jbc.M400798200

Reddy, A., E.V. Caler, and N.W. Andrews. 2001. Plasma membrane repair is mediated by Ca(2+)-regulated exocytosis of lysosomes. *Cell.* 106:157–169. https://doi.org/10.1016/S0092-8674(01)00421-4

Rodríguez, A., P. Webster, J. Ortego, and N.W. Andrews. 1997. Lysosomes behave as $Ca2^{+}$-regulated exocytic vesicles in fibroblasts and epithelial cells. *J. Cell Biol.* 137:93–104. https://doi.org/10.1083/jcb.137.1.93

Rodríguez, A., I. Martinez, A. Chung, C.H. Berlot, and N.W. Andrews. 1999. cAMP regulates Ca2+-dependent exocytosis of lysosomes and lysosome-mediated cell invasion by trypanosomes. *J. Biol. Chem.* 274:16754–16759. https://doi.org/10.1074/jbc.274.24.16754

Sancak, Y., L. Bar-Peled, R. Zoncu, A.L. Markhard, S. Nada, and D.M. Sabatini. 2010. Ragulator-Rag complex targets mTORC1 to the lysosomal surface and is necessary for its activation by amino acids. *Cell.* 141:290–303. https://doi.org/10.1016/j.cell.2010.02.024

Savarino, A., J.R. Boelaert, A. Cassone, G. Majori, and R. Cauda. 2003. Effects of chloroquine on viral infections: an old drug against today's diseases? *Lancet Infect. Dis.* 3:722–727. https://doi.org/10.1016/S1473-3099(03)00806-5

Schatz, G., and B. Dobberstein. 1996. Common principles of protein translocation across membranes. *Science.* 271:1519–1526. https://doi.org/10.1126/science.271.5255.1519

Schindler, A.J., and R. Schekman. 2009. In vitro reconstitution of ER-stress induced ATF6 transport in COPII vesicles. *Proc. Natl. Acad. Sci. USA.* 106:17775–17780. https://doi.org/10.1073/pnas.0910342106

Schlottmann, I., M. Ehrhart-Bornstein, M. Wabitsch, S.R. Bornstein, and V. Lamounier-Zepter. 2014. Calcium-dependent release of adipocyte fatty acid binding protein from human adipocytes. *Int. J. Obes.* 38:1221–1227. https://doi.org/10.1038/ijo.2013.241

Settembre, C., and A. Ballabio. 2014. Lysosomal adaptation: how the lysosome responds to external cues. *Cold Spring Harb. Perspect. Biol.* 6:a016907. https://doi.org/10.1101/cshperspect.a016907

Settembre, C., R. Zoncu, D.L. Medina, F. Vetrini, S. Erdin, S. Erdin, T. Huynh, M. Ferron, G. Karsenty, M.C. Vellard, et al. 2012. A lysosome-to-nucleus signalling mechanism senses and regulates the lysosome via mTOR and TFEB. *EMBO J.* 31:1095–1108. https://doi.org/10.1038/emboj.2012.32

Stoorvogel, W., V. Oorschot, and H.J. Geuze. 1996. A novel class of clathrin-coated vesicles budding from endosomes. *J. Cell Biol.* 132:21–33. https://doi.org/10.1083/jcb.132.1.21

Tang, Z., C. Xia, R. Huang, X. Li, W.C. Wang, W. Guo, L. Duan, W. Luo, D. Cao, and D.X. Luo. 2014. Aldo-keto reductase family 1 member B8 is secreted via non-classical pathway. *Int. J. Clin. Exp. Pathol.* 7:3791–3799.

Tapper, H., and R. Sundler. 1990. Role of lysosomal and cytosolic pH in the regulation of macrophage lysosomal enzyme secretion. *Biochem. J.* 272:407–414. https://doi.org/10.1042/bj2720407

Tapper, H., and R. Sundler. 1995. Bafilomycin A1 inhibits lysosomal, phagosomal, and plasma membrane H(+)-ATPase and induces lysosomal enzyme secretion in macrophages. *J. Cell. Physiol.* 163:137–144. https://doi.org/10.1002/jcp.1041630116

Thomé, R., S.C. Lopes, F.T. Costa, and L. Verinaud. 2013. Chloroquine: modes of action of an undervalued drug. *Immunol. Lett.* 153:50–57. https://doi.org/10.1016/j.imlet.2013.07.004

Tso, A.W., A. Xu, P.C. Sham, N.M. Wat, Y. Wang, C.H. Fong, B.M. Cheung, E.D. Janus, and K.S. Lam. 2007. Serum adipocyte fatty acid binding protein as a new biomarker predicting the development of type 2 diabetes: a 10-year prospective study in a Chinese cohort. *Diabetes Care.* 30:2667–2672. https://doi.org/10.2337/dc07-0413

van Dam, E.M., and W. Stoorvogel. 2002. Dynamin-dependent transferrin receptor recycling by endosome-derived clathrin-coated vesicles. *Mol. Biol. Cell.* 13:169–182. https://doi.org/10.1091/mbc.01-07-0380

Wu, L.E., D. Samocha-Bonet, P.T. Whitworth, D.J. Fazakerley, N. Turner, T.J. Biden, D.E. James, and J. Cantley. 2014. Identification of fatty acid binding protein 4 as an adipokine that regulates insulin secretion during obesity. *Mol. Metab.* 3:465–473. https://doi.org/10.1016/j.molmet.2014.02.005

Xu, A., Y. Wang, J.Y. Xu, D. Stejskal, S. Tam, J. Zhang, N.M. Wat, W.K. Wong, and K.S. Lam. 2006. Adipocyte fatty acid-binding protein is a plasma biomarker closely associated with obesity and metabolic syndrome. *Clin. Chem.* 52:405–413. https://doi.org/10.1373/clinchem.2005.062463

Yamamoto, A., Y. Tagawa, T. Yoshimori, Y. Moriyama, R. Masaki, and Y. Tashiro. 1998. Bafilomycin A1 prevents maturation of autophagic vacuoles by inhibiting fusion between autophagosomes and lysosomes in rat hepatoma cell line, H-4-II-E cells. *Cell Struct. Funct.* 23:33–42. https://doi.org/10.1247/csf.23.33

Zhang, M., and R. Schekman. 2013. Cell biology. Unconventional secretion, unconventional solutions. *Science.* 340:559–561. https://doi.org/10.1126/science.1234740

Zhang, M., S.J. Kenny, L. Ge, K. Xu, and R. Schekman. 2015. Translocation of interleukin-1β into a vesicle intermediate in autophagy-mediated secretion. *eLife.* 4:e11205. https://doi.org/10.7554/eLife.11205